

Review

Research Progress in Electrospray Deposition Coatings on Titanium Alloy Surfaces: A Short Review

Jinfang Wang^{1,2}, Meng Zhang^{1,2} , Sheng Dai^{1,2} and Liu Zhu^{1,2,*} 

¹ Zhejiang Provincial Key Laboratory for Cutting Tools, Taizhou University, Taizhou 318000, China; wjf0909@tzc.edu.cn (J.W.); cailiao@126.com (M.Z.); sdai@tzc.edu.cn (S.D.)

² School of Materials Science and Engineering, Taizhou University, Taizhou 318000, China

* Correspondence: zhuliu@tzc.edu.cn

Abstract: The development process of electrospray deposition (ESD) technology is reviewed, and the principles and differences of ESD technology are discussed in this review. Based on the research status regarding the ESD of titanium alloys, the promotion effect of ESD technology on wear resistance, corrosion resistance, oxidation resistance at high temperatures, and the biocompatibility of titanium alloys was elaborated on. For example, with the use of ESD technology to prepare Ti–Al, TiN, Ni–Cr, and other hardening coatings with high hardness, the maximum hardness of the deposited layer is six times higher than that of the substrate material, which greatly reduces the loss of the material surface in the process of friction in service, and has a high wear–resistance effect. The preparation of a single–phase lamellar coating is more beneficial for improving the oxidation resistance of the substrate. Carbide and a nano–porous coating can effectively enhance the bone integration ability of implants and promote biocompatibility. The application of ESD technology in the surface modification of titanium alloys is reviewed in detail. Finally, the development direction of ESD technology for titanium alloys is proposed.

Keywords: titanium alloy; electrospray deposition; wear resistance; corrosion resistance; high–temperature oxidation resistance; biocompatibility



Citation: Wang, J.; Zhang, M.; Dai, S.; Zhu, L. Research Progress in Electrospray Deposition Coatings on Titanium Alloy Surfaces: A Short Review. *Coatings* **2023**, *13*, 1473. <https://doi.org/10.3390/coatings13081473>

Academic Editor: Michał Kulka

Received: 20 July 2023

Revised: 10 August 2023

Accepted: 18 August 2023

Published: 21 August 2023



Copyright: © 2023 by the authors. Licensee MDPI, Basel, Switzerland. This article is an open access article distributed under the terms and conditions of the Creative Commons Attribution (CC BY) license (<https://creativecommons.org/licenses/by/4.0/>).

1. Introduction

Titanium alloys possess advantages such as low density, high strength–to–weight ratio, low elastic modulus, good fatigue and toughness properties, excellent corrosion resistance, and biocompatibility [1,2]. They are widely used in various fields, including aerospace [3], the automotive and marine industries [4,5], petrochemical industry [6], and in biomedical applications [7]. However, the limitations of titanium alloys, such as low surface hardness, high chemical reactivity, poor wear resistance, and limited high–temperature oxidation resistance, hinder their development and application [8,9]. Therefore, improving the surface properties of titanium alloys to broaden their application range has become one of the current research focuses.

In recent years, researchers both domestically and internationally have employed techniques such as electroplating, micro–arc oxidation, ion spraying, chemical vapor deposition (CVD), physical vapor deposition (PVD), and laser surface treatment to enhance the surface of titanium alloys, achieving significant results. However, the aforementioned methods either make it difficult to obtain modified coatings with a high adhesion strength or lead to the deterioration of the mechanical properties of thin–walled titanium alloy components and are also very costly [10]. Electrospray deposition (ESD) technology is a non–contact processing technique that is not affected by the hardness or thermal properties of the workpiece material [11]. It boasts advantages such as having a simple process, low cost, low residual stress, no deformation, a fast cooling rate ($10^5\sim 10^6$ K/sec) [12], and high adhesion between the deposited layer and the substrate, making it widely used for the surface strengthening of titanium alloy components [13,14].

Therefore, this article reviews the research on ESD technology, starting from its principles. It covers the composition of deposited layers for functional coatings, strengthening mechanisms, technical applications, as well as the main drawbacks and improvement measures of this technology. Furthermore, it provides an outlook on the future development direction and trends of ESD technology on titanium alloy surfaces.

2. Electrospark Deposition Technology

2.1. Overview of Electrospark Deposition Technology

The origins of ESD technology can be traced back to the 1960s when the concept of “electric spark machining” was proposed by a Soviet couple, the Lazarenkos. In the early 1970s, the Central Electric Research Institute in the Soviet Union developed a series of ESD equipment [15]. In the 1980s, Lazarenko’s theory was put into practice by the Institute of Applied Physics of the Soviet Union’s Moldavian Academy of Sciences, leading to the development of the 3H series of equipment, which was successfully applied in industrial fields [16]. With the rapid development of industrial equipment, the experimental factory of the Institute of Applied Physics in Moldova started using new ESD equipment with thyristors and transistors, significantly improving the operability of the equipment and the quality of the deposited layers on the components. By the 1990s, the Soviet Union had greatly reduced production costs by employing this equipment, with 37 units alone saving nearly RUB 400,000 [17].

The research on ESD technology in China started in the 1960s when a batch of ESD equipment was developed. However, limited conditions at that time hindered its promotion and application. With the development of industrialization in China, mechanical equipment units in Tianjin, Shandong, and other regions began to conduct in-depth research on ESD technology due to its promising applications in tools and molds [18]. Scholars in Jiangsu, Zhejiang, and other areas have also made significant contributions to the research on the strengthening mechanisms, process applications, and equipment aspects of this technology. In the early 1980s, ESD technology was designated as a new process promotion project by the former Ministry of Machinery Industry and listed as a key new technology for promotion in the Sixth Five-Year Plan by the National Economic Commission. Tsinghua University and Shenyang University of Technology have achieved certain results in developing new strengthening equipment and processes, leading to increased attention being paid to this technology domestically [19,20]. In the early stages of research, ESD technology in China was mainly applied to the surface strengthening treatment of molds, tools, and other mechanical components [21], and was widely used in industries such as machinery manufacturing and agricultural machinery [22]. In addition to research on corrosion resistance, wear resistance, and the performance of composite coatings using ESD, there are also reports on thermal barrier coatings [23] and flame-retardant coatings [24]. ESD technology not only effectively improves the surface properties of tooling and molds, such as thermal conductivity, wear resistance, corrosion resistance, and surface hardness, but also offers advantages over conventional surface treatment methods, including easy equipment portability, flexible usage, and low cost.

Currently, domestic research on ESD technology in China primarily focuses on improving the corrosion resistance and wear resistance of materials, while there is relatively little research on using ESD technology to enhance the heat resistance, oxidation resistance (thermal barrier coatings and flame-retardant coatings), and biocompatibility of material surfaces. Therefore, it is necessary to have a balanced focus in future research on ESD technology and fully exploit its unique advantages so that ESD technology can find wider applications in various fields.

2.2. Principle of Electrospark Deposition Technology

The ESD technique utilizes the pulsed spark discharge between the metal substrate and the electrode, enabling the electrode material to melt and infiltrate into the surface layer of the metal substrate under high temperature ($5 \times 10^3 \sim 2 \times 10^4$ °C) and high pressure,

forming a surface–alloyed deposition layer with special properties and metallurgical bonding to the substrate [25,26]. This treatment optimizes the physicochemical properties of the substrate surface and improves the hardness, wear resistance, and corrosion resistance of the original substrate material to a certain extent [27]. Figure 1 illustrates the working principle of the ESD technique. The ESD technique involves highly complex physical, chemical, energy conversion, and thermodynamic reactions [28]. It is challenging to systematically study the transient ($10^{-6}\sim 10^{-5}$ s) discharge effects, which poses certain obstacles to the research on the film formation mechanism of ESD technology [29]. However, researchers continue to explore and study the process's shortcomings and improvement methods.

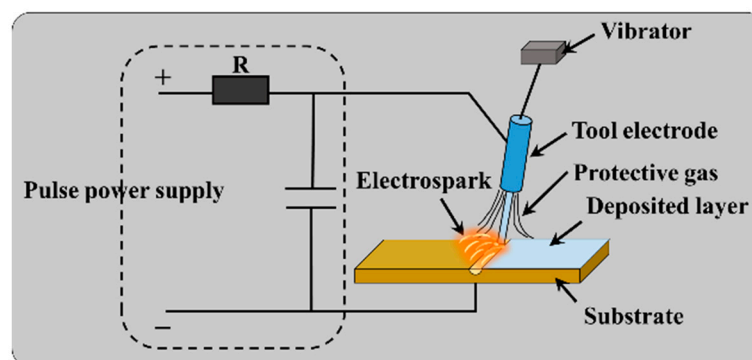


Figure 1. Schematic diagram for principles of ESD technique.

Currently, researchers mainly categorize the discharge processes of ESD technology into two types: spark discharge [30–32] and arc discharge [33,34]. In the case of spark discharge, the essence lies in bringing the working electrode close to the substrate, where high–density thermal energy is generated at the discharge site, causing the instant melting of the electrode material and deposition onto the substrate surface, thereby achieving the surface reinforcement of the substrate. The ESD technique can be classified into two types: contact discharge and non–contact discharge. Non–contact discharge refers to maintaining a certain distance between the working electrode and the target substrate, resulting in an increasing electric field strength leading to dielectric breakdown and spark discharge. During the discharge process, thermal energy is generated by the impact of electrons on the electrode surface, resulting in the melting of the electrode material and the formation of electrode droplets. These droplets form a particle stream, leading to the stable deposition of the electrode material on the substrate surface, forming a stable electrode thin–film strengthening layer [30]. In contrast to non–contact discharge, contact discharge involves the generation of a large instantaneous current through localized electrode–substrate contact. This current results in a substantial high temperature, leading to splashing on the substrate surface. By utilizing this process, the electrode material is melted at high temperatures, and, after absorbing a certain amount of energy, splashing occurs, ultimately depositing the material onto the target substrate surface and forming a robust metallurgical layer with the substrate [31]. Arc discharge, similar to contact discharge in spark discharge, essentially involves the generation of instantaneous high temperatures between the electrode and the substrate, resulting in the melting of the electrode material. However, in contrast, arc discharge generates a plasma arc between the substrate and the electrode during the pulse process, thereby melting the electrode material to strengthen the surface of the substrate. Due to the short discharge time and the dissipation of generated heat, arc discharge has a minimal impact on the substrate and does not cause significant damage to the material's inherent properties [33,34]. However, besides these two main types of ESD discharge, some researchers consider ESD technology a hybrid process that combines various techniques such as welding, vapor deposition, and metal overlay. This hybrid process primarily consists of three steps: (1) electrode–substrate contact, resulting in the generation of heat due to the discharge; (2) rapid movement of the

electrode, igniting the arc; (3) the melting of the electrode material and the formation of metallurgical bonding between the electrode and the substrate [31].

Regardless of the discharge method used, the goal is to enhance the surface of the substrate material by applying ESD technology. Due to the complexity of the principles underlying ESD technology, researchers have not yet reached a clear consensus on the specific discharge mechanisms. Therefore, summarizing and conducting in-depth research on ESD technology will provide valuable insights for further investigation and understanding of the technique.

3. Titanium Alloys Electrospark Deposition Coating

The ESD layer is not a simple electrode substrate accumulation but a product generated via alloying reactions between the electrode and the substrate in the micro-scale discharge zone. The products consist of diverse compounds, each with their own unique properties, directly influencing the coating's microstructure and organization, thereby affecting the material's performance. To improve the cavitation erosion and wear resistance of water pump flow components, Zhang et al. [35] employed electric spark technology to prepare a WC-8Co metal layer on the surface of stainless steel. The experimental results showed that the metal layer was uniform, continuous, and dense, without significant cracks or voids, and that there was no distinct boundary between the metal layer and the substrate material, indicating metallurgical bonding. The highest microhardness of the metal layer was $HV_{0.3} = 18,920$ MPa, with an average hardness of $HV_{0.3} = 17,950$ MPa, approximately six times that of the substrate hardness (2600 MPa). The wear resistance was 3.75 times higher than that of the substrate. The significant performance improvement is attributed to the metal deposition layer prepared using ESD technology. Therefore, the targeted deposition of different metal layers can achieve performance enhancement for substrate components. Burkov et al. [36] prepared Ti-Al intermetallic compound coatings on the surface of a Ti-6Al-4V alloy by employing electric spark treatment in a mixture of Ti and Al particles. With an increase in the concentration of Al in the particle mixture, the phase composition of the corresponding coating changed from titanium-rich aluminide (Ti_3Al) to aluminum-rich aluminide ($TiAl_3$). The high-temperature oxidation resistance [37], microhardness [38], and corrosion resistance [39] of the coating samples were significantly improved.

Clearly, electrical discharge deposition technology significantly optimizes the performance of titanium alloys, and the deposition of different reinforcement layers expands the range and depth of applications in various fields. Therefore, researchers have conducted extensive studies on applying electrical discharge deposition technology to enhance different performance aspects of titanium alloys. Currently, the technology is commonly used in the preparation of coatings for surface wear resistance, corrosion resistance, high-temperature oxidation resistance, and for the biocompatibility of components [40].

3.1. Microstructure

The organization and structure of electrical discharge deposition coatings are often influenced by the process and deposition materials. They not only affect the interdiffusion process between the substrate and the coating but also the extent of diffusion. The structure of the deposition layer affects the performance of the material after surface modification. For example, the microhardness of the WC-modified layer can reach up to 950.7 $HV_{0.2}$, while the microhardness of the NiCr-modified layer is the lowest. The trend in hardness variation indicates the presence of a transitional region between the deposition layer and the substrate. Additionally, the performance of the deposition layer is also influenced by stress. The residual stress distribution in the deposition layer is non-uniform, with both tensile and compressive stress present. Residual compressive stress enhances the fatigue strength of the modified layer and suppresses the generation of fatigue cracks, while residual tensile stress has the opposite effect. In summary, there is a certain relationship between the organization, structure, and performance of the deposition layer in the electrical discharge surface

modification of titanium alloys. Understanding these relationships helps to optimize the preparation process of the deposition layer and improve the quality of the modified layer.

Liu et al. [41] used electrical discharge deposition to prepare Ti–Al intermetallic compound coatings on the surface of a Ti–6Al–4V alloy. Through investigations of the coating's chemical state, microstructure, phase composition, microhardness, and surface residual stress, they discovered many new Ti–Al intermetallic compounds different from the deposition material formed, along with a small amount of Al_2O_3 in the coating. The high energy of electrical discharge promotes interdiffusion and chemical reactions between the elements. Figure 2 shows the cross-sectional microstructure and elemental distribution. It can be seen that the Al element and Ti element have obvious mutual diffusion behavior from the coating to the substrate, and the diffusion zone is 5 μm , that is, from the coating at 10 μm to the titanium substrate at 15 μm . Wang et al. [24] investigated the feasibility of using the electrical discharge deposition process to prepare Ti–Cu flame-retardant coatings. The Ti–Cu coating surface exhibits a typical splatter appearance, with different compositions and phases within individual splatters. The coating structure presents a river-like and hilly-valley-like morphology, featuring numerous nanoscale porosities and trumpet-shaped splatters. Tensile residual stress in the Ti–Cu coating leads to longitudinal cracks terminating at the interfaces. Secondary layers with layer-layer interfaces are present in the coating. Moreover, the Ti–Cu coating is primarily composed of Ti_3Cu , Ti_2Cu , $\text{Ti}_{3.3}\text{Al}$, and Ti, with a hardness of $760 \text{ HV}_{0.05/10}$, greatly improving the surface performance of the substrate.

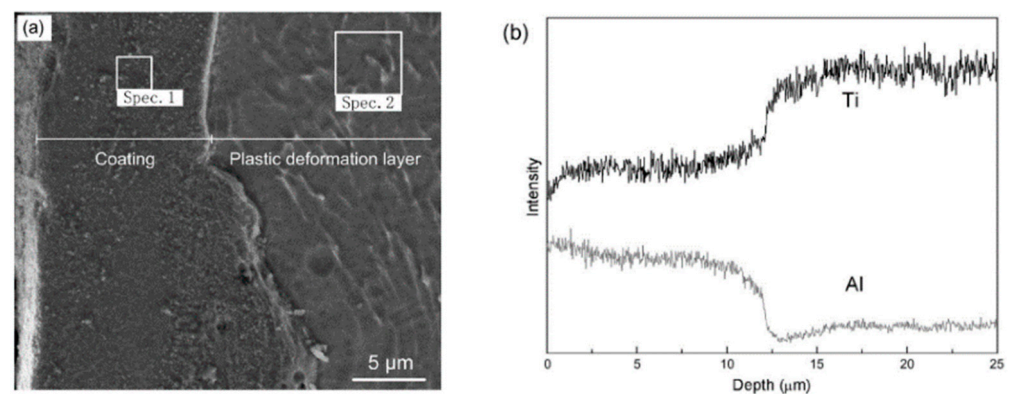


Figure 2. (a) Cross-sectional microstructure and (b) titanium/aluminum distribution along the depth direction of the Ti–6Al–4V alloy. Reprinted with permission from Ref. [41] Copyright 2015 Elsevier.

Hassan et al. [42] used the ESD technique to prepare Ti–TiB–TiB₂ coatings on a Ti–6Al–4V substrate. The microstructure of the coatings was analyzed using scanning electron microscopy (SEM) and energy-dispersive spectroscopy (EDS). A comparison of the microstructure of the coating with that of the electrode indicated that the coating exhibits a finer microstructure than the electrode, primarily due to the high solidification rate during the ESD process. The predominant phases in the microstructure of the coatings in Figure 3a,b are needle-like TiB and granular TiB₂ dispersed in the Ti matrix. By reducing the input power from 110 W to 40 W to increase the solidification rate, the microstructure of the coatings becomes finer. In this case, TiB₂ and TiB phases with nanoscale sizes are dispersed in the Ti matrix.

E.I. Zamulaeva et al. [43] used the pulse electrical spark deposition (PESD) technique and a Cr_2AlC electrode material (EM) to obtain coatings with a significant amount of MAX phases (represent a family of ternary carbide or nitride compounds of the general formula $\text{M}_{n+1}\text{AX}_n$, where $n = 1, 2, 3$; M is an early transition metal; A some Group IIIA or IVA element; and X = C and/or N) on a Ti substrate. The structure and phase formation of the coatings generated in different modes were investigated. In the initial stage of PESD, a layer of titanium carbide was formed at the interface due to the chemical reaction between the Cr_2AlC electrode and Ti substrate, further serving as a diffusion barrier. When deposited in

a low-energy mode in an Ar atmosphere, the TiC layer continued to grow throughout the process, consuming the MAX phase in this reaction. In the high-energy mode, in the case of PESD under an argon atmosphere, the titanium carbide layer developed rapidly, further acting as a diffusion barrier and corrosion-resistant cathode. Cr_2AlC became the dominant phase in the coating. Importantly, by carrying out the process in a protective atmosphere and selecting a strong carbide-forming metal as the substrate for the deposited coating to minimize any chemical interaction with atmospheric oxygen, the deposited coating consisted mainly of MAX phases. R.J. Wang et al. [44] used the ESD technique to deposit WC92–Co8 cemented carbide on a titanium alloy surface. A thick and dense coating with rare cracks was obtained, as shown in Figure 4, i.e., the cross-sectional microstructure of the WC92–Co8 coating on the titanium alloy surface. Metallurgical bonding was formed between the coating and the substrate due to the mixing of WC92–Co8 with the titanium alloy at localized melt pools and interfaces. Titanium elements migrated into the coating and underwent a chemical reaction with carbon. Stable phases such as TiC, W_2C , and W were present in the coating. The thermodynamic analysis and experimental results suggest the possible formation of intermediate phases in the coating.

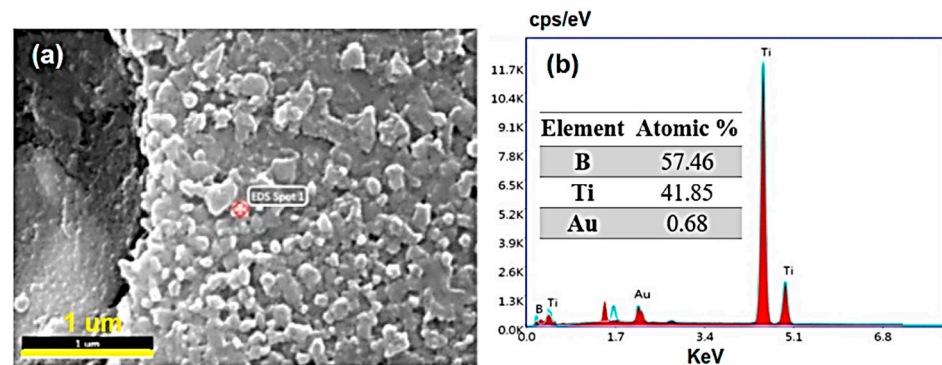


Figure 3. (a) SEM image and (b) EDS spectra showing the presence of TiB_2 particles around the pores. Reprinted with permission from Ref. [42] Copyright 2020 Elsevier.

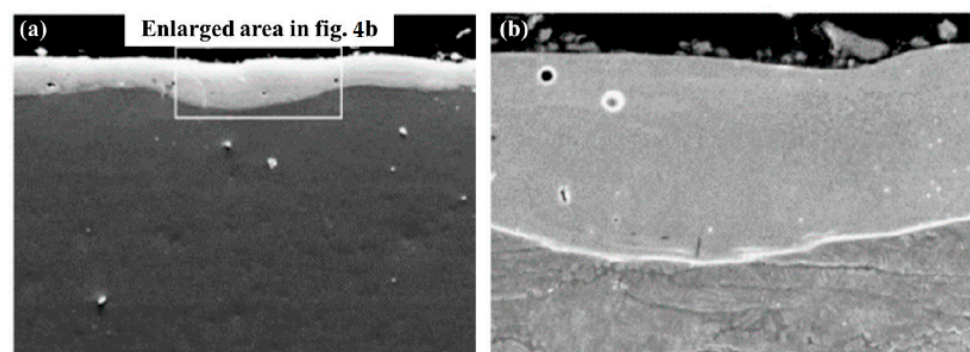


Figure 4. SEM cross-section images of WC92–Co8 coating on Ti alloy. (a) Macroscopic view; (b) enlarged area. Reprinted with permission from Ref. [44] Copyright 2004 Elsevier.

Hong et al. [45] utilized the ESD technique to prepare Zr-based amorphous–nanocrystalline coatings on a TC11 titanium alloy surface. Figure 5 shows the TEM image and electron diffraction pattern of a selected region in the amorphous–nanocrystalline coating. The coating mainly consists of amorphous phase $\text{Zr}_{55}\text{Cu}_{30}\text{Al}_{10}\text{Ni}_5$, with a distribution of numerous nanoscale particles such as CuZr_3 , Ni_2Zr_3 , NiZr_2 , with particle diameters ranging from 2 to 4 nm. The alloy system composed of a Zr-based electrode material and TC11 substrate exhibits a strong ability to form an amorphous phase, and in the rapid heating and cooling process of ESD, the amorphous phase transforms into the nanocrystalline phase. The long-range diffusion of Zr, Cu, and other atoms in the amorphous structure

plays a crucial role in the nucleation and growth of nanoscale phases. The coating is dense, uniform, and metallurgically bonded to the TC11 substrate.

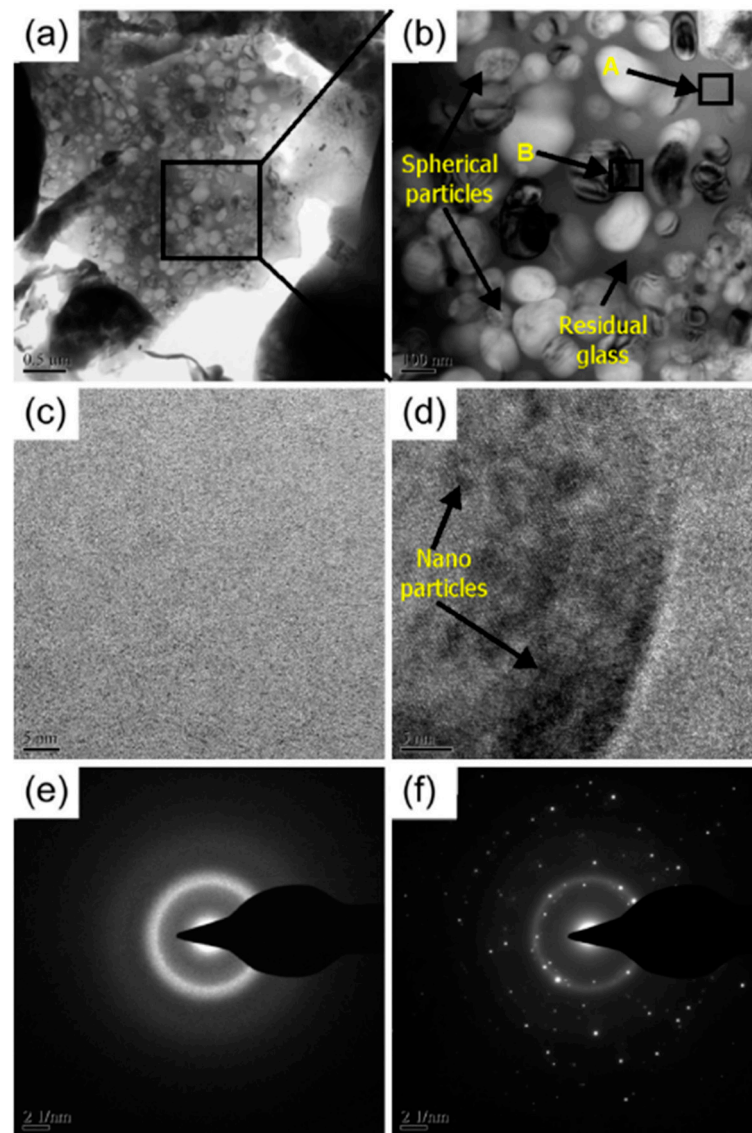


Figure 5. TEM images and selected area electron diffraction patterns of the coating: (a) TEM bright field image; (b) magnified view of (a); (c) HRTEM image of area A in (b); (d) HRTEM image of area B in (b); (e) electron diffraction patterns of area A in (b); and (f) electron diffraction patterns of area B in (b). Reprinted with permission from Ref. [45] Copyright 2015 Elsevier.

3.2. Wear Resistance

As is well known, titanium alloys have a low hardness, high friction coefficient, and poor wear resistance. When used as sliding components, they are prone to adhesive wear with other materials, leading to early failure and limiting the breadth and depth of titanium and its alloys' applications [46]. Therefore, improving the wear resistance of titanium alloys has become an urgent issue in titanium alloy research. Kiryukhantsev et al. [47] combined the advantages of magnetron sputtering and ESD techniques and compared single-layer Ti alloy coatings with double-layer Ti alloy coatings. The results showed that the double-layer Ti alloy structure, prepared by combining the two techniques, exhibited excellent wear resistance compared to the deposited single-layer Ti alloy coating. Figure 6 presents the dependence of the coefficient of friction (CoF) on the sliding distance during the frictional testing of ESD, MS, MS-ESD, and MS-ESDpol coatings on a 440 C ball under a normal load

of 1 N. The figure also shows the characteristic wear marks on the corresponding material surfaces (samples 1, 2, 3, and 4) and the microphotographs of the worn regions (coatings 2 and 3). The significant improvement in wear performance is attributed to the metallurgical bonding between the metal layer prepared using the ESD technique and the substrate, which prevents coating failure and subsequent component failure during use. This result provides favorable evidence for the advantages and prospects of ESD technology.

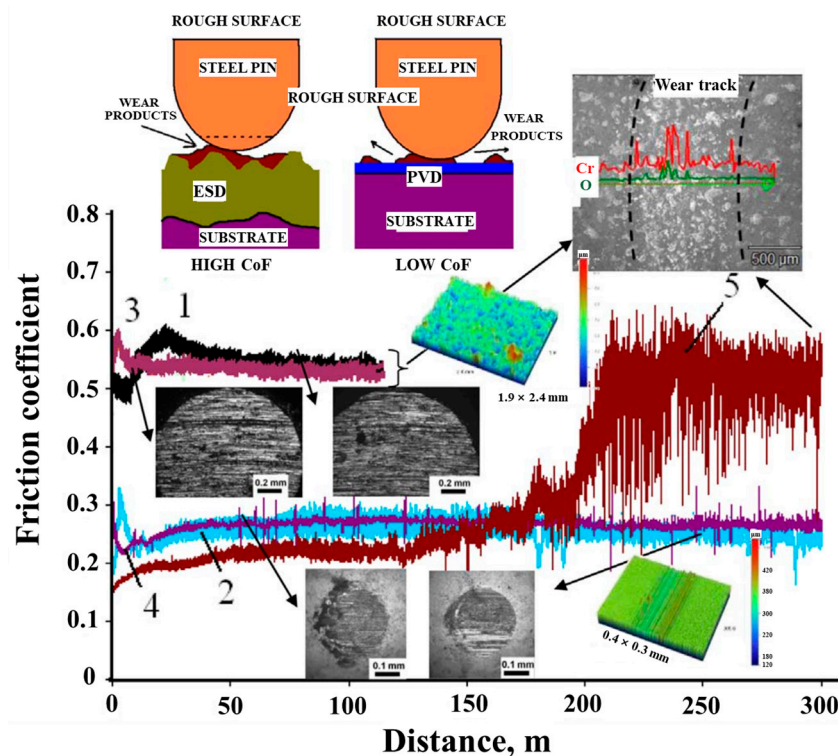


Figure 6. Friction coefficients and sliding distance with corresponding SEM and optical profilometry images of tribological contact areas. Scheme illustrating the different wear behavior of ESD and MS coatings. 1—ESD ($R_a = 8 \mu\text{m}$), 2—MS ($R_a = 0.05 \mu\text{m}$), 3—MS—ESD ($R_a = 8 \mu\text{m}$), 4—MS—ESDpol ($R_a = 0.1 \mu\text{m}$), and 5—ESDpol ($R_a = 0.1 \mu\text{m}$). Reprinted with permission from Ref. [45] Copyright 2018 Elsevier.

At present, to enhance the wear resistance of material surfaces using ESD technology, high-hardness materials such as tungsten carbide–cobalt alloy (WC–Co) and nickel–based alloys are commonly selected as electrodes [44]. These materials are deposited onto the substrate surface using ESD, forming a low friction coefficient and a high hardness reinforcement coating. The purpose is to achieve a coating hardness several times higher than that of the substrate, greatly reducing the material surface wear during friction in service, and achieving high wear resistance. For example, Sun et al. [48] used ESD to deposit NiCr coatings with a thickness of 40–70 μm on a TA2 substrate and studied their frictional performance. The research showed that the NiCr coatings had fewer defects such as cracks and pores, and the maximum hardness of the coatings was 620 HV, significantly higher than that of the substrate, resulting in improved wear resistance. Burkov et al. [36] prepared Ti–Al intermetallic compound coatings on Ti–6Al–4V alloy surfaces using ESD. Figure 7 shows the microhardness of the coatings and the wear rate analysis under different loads. The wear rate of the coatings decreased with an increase in aluminum concentration, and it decreased with an increase in titanium content. The microhardness of the coatings ranged from 6.4 to 9.4 GPa, with the coatings having a molar ratio of titanium to aluminum close to unity exhibiting the highest hardness. The coatings showed a wear resistance 4–27 times higher than the initial alloy when subjected to dry sliding under a load of 10 N and 6–36 times higher under a load of 25 N.

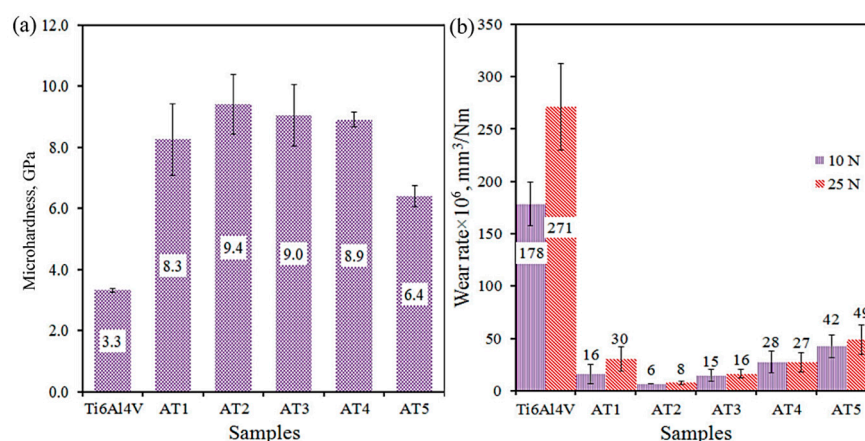


Figure 7. Microhardness (a) and wear rate (b) of samples. Reprinted with permission from Ref. [36] Copyright 2020 Elsevier.

As already mentioned, Liu et al. [41] conducted a study using the electrical spark deposition (ESD) technique to prepare Ti–Al intermetallic compound coatings with a thickness of 12 μm on the surface of a Ti–6Al–4V alloy. The deposited coatings were primarily composed of Ti–Al intermetallic compounds, with a small amount of Al_2O_3 . Additionally, the experimental results demonstrated a significant improvement in the microhardness of the coatings. The coatings exhibited a metallurgical bond with the plastic deformation layer, and a plastic deformation layer was observed within the coatings. The formation of new Ti–Al intermetallic compound phases within the coatings was attributed to the high-energy electrical sparks during the deposition process, which promoted chemical reactions between the electrode and substrate elements. This finding highlights the significant enhancing effect of Ti–Al intermetallic compound coatings on hardness and wear resistance in titanium alloys. Liu et al. [49] prepared reinforcement coatings on titanium alloy surfaces using NiCr–3 as the electrode. They analyzed the influence of process parameters on the surface roughness, morphology, and thickness of the coatings, as well as the changes in the microstructural organization of the coatings under different process conditions. The results showed that the coating thickness initially increased and then decreased with an increase in the deposition time ratio, with the optimal deposition time ratio being 4 min/cm^2 . An increase in the deposition frequency resulted in a decrease in the number of surface cracks. With an increase in the deposition voltage, deposition frequency, and deposition time ratio, the hardness of the coatings continuously increased and eventually stabilized. TiN (titanium nitride) coatings possess excellent properties such as high hardness, high strength, low friction coefficient, wear resistance, and corrosion resistance, making them promising surface reinforcement coatings for titanium alloys. For example, Hao et al. [50] used electrical spark deposition technology to prepare TiN/Ti composite coatings on Ti–6Al–4V surfaces. The average microhardness of the coatings reached 1388 $\text{HV}_{0.1}$, which is more than six times higher than that of the substrate. The coatings exhibited good wear resistance, attributed to the presence of nitrogen defects within the TiN phase, which enhanced the metallic behavior and toughness of the TiN coatings, resulting in excellent wear resistance. Su et al. [51] employed electrical spark deposition to deposit a Ni45 reinforcement coating with a thickness of up to 50 μm on a BT20 titanium alloy substrate. The coating mainly consisted of NiTi, NiTi, and Ti strengthening phases. The surface microhardness of the deposited layer reached 910 $\text{HV}_{0.05}$, approximately 2.7 times higher than that of the substrate. The hardness of the entire cross-section of the deposited layer exhibited a gradient distribution, gradually decreasing from the surface of the coating to the substrate. Hong et al. [1] conducted a systematic study on the influence of the electrical spark deposition process parameters on the microstructure and wear resistance of TiN coatings. The coating's microstructure was characterized using the thickness, TiN content, and porosity. A statistical model was established to identify the important factors

affecting the coating's microstructure and wear resistance. The results showed that the wear mass loss varied with changes in output voltage and nitrogen flow rate due to the alteration of the wear mechanism in TiN coatings. The primary wear mechanisms observed in TiN coatings prepared under the optimal process parameters were micro-cutting wear accompanied by microfracture wear.

The significant increase in the hardness and wear resistance of different titanium alloys after surface modification using ESD techniques is mainly due to the presence of a large amount of high-performance intermetallic compounds in the coatings, such as Ti–Al, TiN, and Ni–Ti, which possess high hardness and excellent wear resistance, thus significantly improving the performance of the treated titanium alloy components. For instance, Liu et al. [52]. developed a process combining ultrasonic impact treatment (UIT) with ESD to fabricate hard wear-resistant coatings on a Ti–6Al–4V substrate. Furthermore, the coatings also contain new phases of titanium carbide nitride and iron titanium oxide, including amorphous and nanocrystalline structures. Additionally, a compressive residual stress field is formed within and beneath the coatings. These factors contribute significantly to the improved wear resistance of the coatings. Figure 8a shows a significant improvement in the wear resistance of samples treated with the combined UIT and electrical spark deposition compared to the wear resistance of the Ti–6Al–4V substrate. Despite the relatively high friction coefficient, the volume loss due to wear is reduced by four orders of magnitude. In Figure 8c, noticeable furrows can be observed on the wear tracks, which are typical features of abrasive wear. From Figure 8d, visible adhesive traces (A) and fragments formed by adhesive wear (B) can be seen. Therefore, the experiment indicates that the coating exhibits excellent wear resistance.

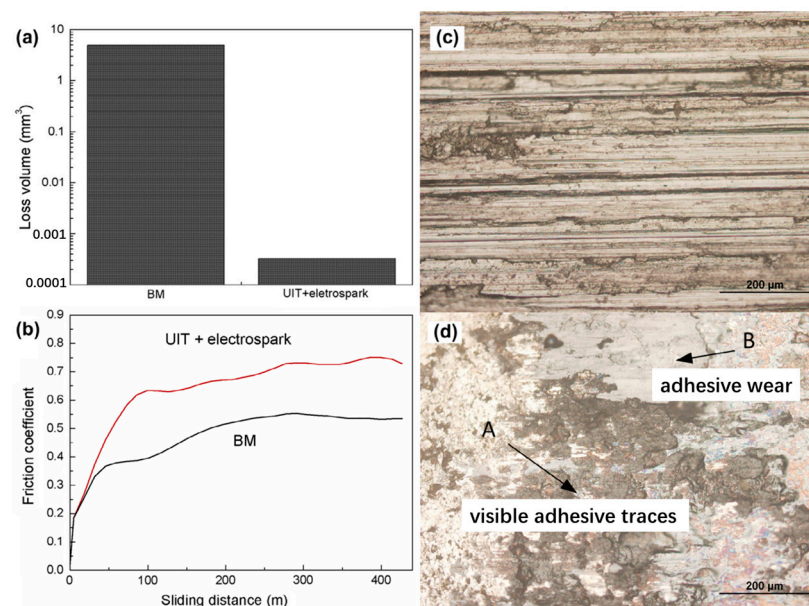


Figure 8. (a) Wear results; (b) friction coefficient; and wear scars (c) on the base material and (d) on the sample treated with combined UIT and electrospark processing. Reprinted with permission from Ref. [52] Copyright 2014 Elsevier.

A. A. Burkov et al. [53] used the ESD technique to deposit a Ti–Ni–Zr–Mo–Al–C composite coating on the surface of a Ti–6Al–4V alloy. The deposited coating has a thickness of approximately 50 μm. The coating composition is represented by AlNi₂Ti, MoNi₄, and NiTi intermetallic compounds. The average roughness (Ra) of the coating is around 3 μm. The microhardness of the deposited layer is three times higher than that of the Ti6Al4V titanium alloy. The friction and wear tests of the Ti–Ni–Zr–Mo–Al–C coating against R6M5 steel showed that the wear resistance of the coating is five times higher than that of the Ti6Al4V alloy. In order to enhance the wear resistance of a titanium alloy, Hong et al. [45]

utilized ESD technique to prepare a Zr-based amorphous–nanocrystalline coating on the surface of a TC11 titanium alloy, and investigated the tribological behavior and mechanisms of the coating. The results indicated that the coating had a thickness of 55–60 μm and an average microhardness of 801.3 $\text{HV}_{0.025}$. The coating exhibited excellent anti-friction and anti-wear properties. As shown in Figure 9a, the friction coefficient of the coating varied between 0.13 and 0.21 with minimal fluctuations, resulting in an approximately 60% reduction compared to the friction coefficient of the TC11 substrate. The wear resistance of the coating was improved by 57% compared to the TC11 substrate, as illustrated in Figure 9b. The predominant wear mechanism of the coating was micro-cutting wear accompanied by oxidative wear.

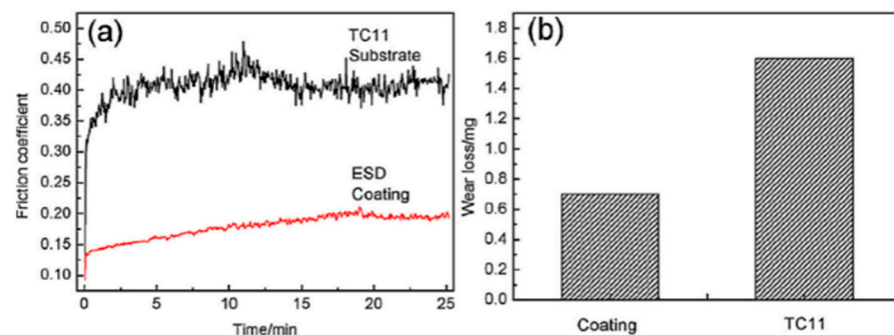


Figure 9. The friction and wear results of the amorphous–nanocrystalline coating and TC11 substrate: (a) friction coefficient; (b) wear losses. Reprinted with permission from Ref. [45] Copyright 2015 Elsevier.

In order to improve the tribological performance of a titanium alloy, Hong et al. [54] employed the ESD technique to deposit in situ TiN coatings on the surface of a TC11 titanium alloy. The influence of nitrogen flux on the microstructure and tribological properties of the TiN coatings was investigated. The results of the friction coefficient and wear volume of the TiN coatings under different nitrogen flux conditions are shown in Figure 10. The results indicated that at a lower nitrogen flux, the coating was thinner and mainly composed of Ti_2N , $\alpha\text{-Ti}$, TiO , and TiN phases. Due to the rapid solidification during ESD, a metastable Ti_2N phase was formed. When the nitrogen flux was too high, a significant amount of microcracks and voids would appear in the coating. Under a moderate nitrogen flux, the coating was predominantly composed of the TiN phase, exhibiting a dense and uniform structure (50–55 μm). The average hardness was $\text{HV}_{0.2}1165.2$, which was 3.4 times higher than that of the TC11 substrate. The TiN coatings prepared under a moderate nitrogen flux demonstrated the best wear resistance. The wear mass loss of the coating was 0.4 mg, which accounted for 2/9 of the TC11 substrate. The primary wear mechanisms of the coating were micro-cutting wear and complex plastic deformation wear.

In order to enhance the wear resistance of a titanium alloy, particularly under high-load friction conditions, Hong et al. [55] employed the ESD technique to prepare composite coatings on the surface of a TC11 titanium alloy. The microstructure of the coating was analyzed, and the fracture toughness and microhardness of the coating were tested. The wear behavior and wear mechanisms of the coating under different load conditions were investigated. The results revealed that the composite coating consisted of a TiN base layer (Coating I) and a Zr-based amorphous–nanocrystalline surface coating (Coating II). The composite coating exhibited a dense structure with a thickness of approximately 90–95 μm , metallurgically bonded to the substrate. The fracture toughness of the composite coating was about 9.36 $\text{MPa}\cdot\text{m}$. The microhardness of the coating exhibited a gradient change. The average microhardness values of Coating I and Coating II were 1221.5 $\text{HV}_{1.96}$ and 801.3 $\text{HV}_{1.96}$, respectively. The wear resistance tests of the TC11 substrate, Coating I, and the composite coating demonstrated excellent wear resistance, particularly under high-load friction conditions (as shown in Figure 11a,b). Under low-friction conditions, the primary

wear mechanisms of the composite coating were micro-cutting wear and repetitive plastic deformation wear. Under high-load friction conditions (>8 N), the predominant wear mechanism of the composite coating was micro-cutting wear, accompanied by partial micro-fracture wear. The average wear rate of the composite coating was approximately 1.2–1.5 times higher than that of the single TiN coating, and about 2.6–2.7 times higher than that of the TC11 substrate.

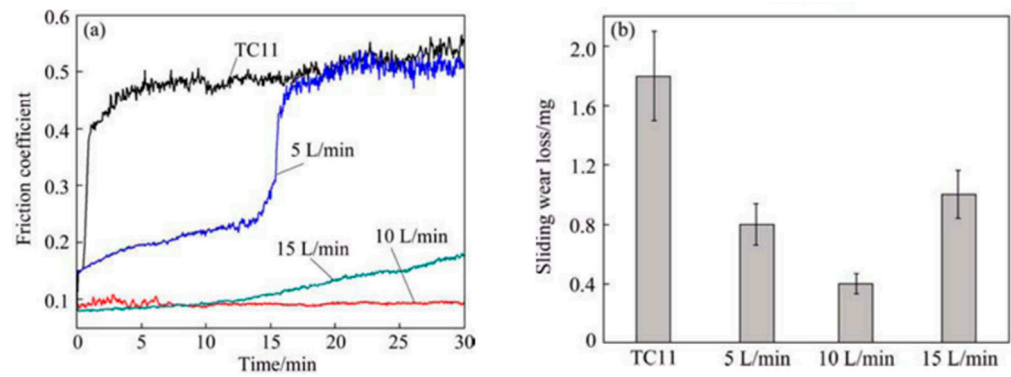


Figure 10. (a) Friction coefficients and wear losses of TC11 substrate, (b) TiN coatings deposited at different nitrogen fluxes. Reprinted with permission from Ref. [54] Copyright 2015 Elsevier.

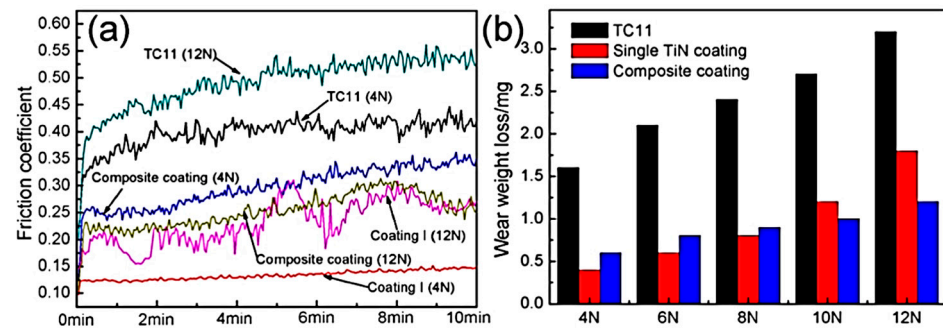


Figure 11. The wear results of TC11 substrate, single TiN coating, and composite coating: (a) friction coefficient curves; (b) wear weight losses. Reprinted with permission from Ref. [55] Copyright 2016 Elsevier.

Li Ping et al. [56] used a silicon bronze (QSi3–1) electrode to perform electrical discharge surface strengthening on a Ti17 titanium alloy in both silicone oil and argon gas. The results showed that using the QSi3–1 electrode with electrical parameters of 30 V and 1500 μ F in argon gas and silicone oil, respectively, resulted in hardened layers with a microhardness up to HV550 and HV494, and thicknesses of approximately 10 μ m and 5 μ m. The former hardened layer consisted mainly of Ti_3Cu and Cu, with small amounts of TiSi_2 and Ti, while the latter hardened layer was composed of Ti_3Cu and Cu phases, along with minor amounts of TiO, TiN, and Ti_3SiC_2 phases. Under dry ring-on-disc friction and wear conditions at a sample rotation speed of 200 r/min, the wear of the hardened samples in argon gas and silicone oil was only 1/56 and 1/24 of that of the titanium alloy substrate, respectively. The titanium alloy substrate mainly experienced oxidative and adhesive wear, while the wear of the surface-modified layer was attributed to the detachment of the hardened layer causing abrasive wear. Sun et al. [48] used electrical discharge deposition technology with a NiCr alloy electrode to prepare a continuous and uniform NiCr/Ti composite coating on the surface of the TA2 substrate. The coating thickness was approximately 40–70 μ m. The coating formed new phases such as NiTi_2 , $\text{Cr}_4\text{Ni}_{15}\text{Ti}$, $\text{Cr}_{1.75}\text{Ni}_{0.25}\text{Ti}$, and NiTi, indicating that the coating had achieved the surface modification of the substrate. The hardness of the coating decreased with increasing distance from the surface, and the coating exhibited the highest hardness at a distance of 10 μ m from

the surface, reaching HV620. The coating demonstrated high wear resistance. Prakash et al. [57] employed a method of adding Si powder to the electrical discharge machining fluid to perform electrical discharge alloying on β -Ti implants. A bioceramic hard layer was prepared using the scanning probe microscopy–electron scanning microscopy (SPM–ESA) technique. By forming a 15 μm thick recast layer on the surface of the β -Ti implants, mainly composed of TiO_2 , ZrO_2 , SiO_2 , TiC , and SiC oxides and carbides, the microhardness of the β -Ti implants was increased from 380 HV to 1080 HV. Figure 12a,b presents the coefficient of friction (COF) and specific wear rate of the frictional properties of the unprocessed and SPM–ESA–processed surfaces. The friction and wear test results showed that surface active agents could reduce the coefficient of friction, and decrease the wear volume and specific wear rate of the β -Ti implants, thereby improving their tribological performance. Under dry friction conditions, compared to the untreated samples, the friction coefficient decreased by 60%, and the wear rate increased by 29 times.

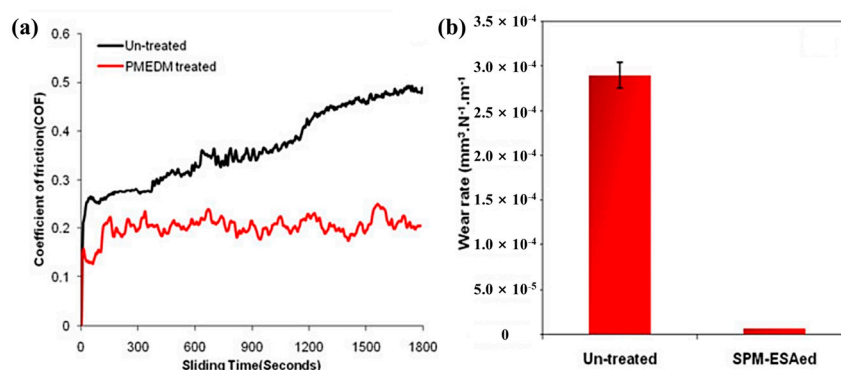


Figure 12. (a) COF curves and (b) specific wear rate for untreated and SPM–ESA treated β -Ti implant. Reprinted with permission from Ref. [57] Copyright 2017 Elsevier.

3.3. Corrosion Resistance

During application, titanium alloys inevitably experience component failures such as hydrogen embrittlement, corrosion fatigue, and stress corrosion cracking. Spark deposition technology can produce corrosion-resistant coating surfaces, which mainly depend on the physicochemical properties of the oxide film formed on the coating surface and the heterogeneity of the surface structure [58]. The improvement in corrosion resistance is mainly attributed to the uniform surface microstructure and the absence of grain boundaries [59]. Coatings with high corrosion potential and low corrosion current density exhibit lower corrosion rates, thus demonstrating excellent corrosion resistance on the coating surface. Research has shown that titanium (Ti) and its alloys exhibit excellent corrosion resistance in HNO_3 due to the formation of protective and self-adherent oxide films [60]. Burkov et al. [36] used the spark deposition technique to form Ti–Al intermetallic compound coatings on a Ti–6Al–4V alloy utilizing a mixture of titanium and aluminum particles. Figure 13 depicts the polarization curves of different coating samples in a 3.5% NaCl solution. The results indicate that samples with a higher aluminum content (AT3–AT5) exhibit higher polarization resistance values and corrosion potentials. Samples with a higher titanium content (AT1–AT2) have lower R_p and comparable corrosion potentials, indicating that coatings with higher aluminum content possess good corrosion resistance.

Teplenko et al. [61] deposited AlN-ZrB_2 coatings with ZrSi_2 additives on the surface of a BT6 titanium alloy using spark deposition technology. The experimental results showed that the formed Al_2SiO_5 and ZrSiO_4 phases in the coating acted as lubricants, and under the optimal process parameters, the friction coefficient of the deposited layer could reach 0.13. At a load of 2.56 MPa and a sliding velocity of 14 m/s, the corrosion wear rate was 6 $\mu\text{m}/\text{km}$, effectively improving its wear resistance and corrosion wear resistance. Tang et al. [62] conducted surface strengthening treatment on a titanium alloy using spark deposition technology. The experimental results revealed a significant improvement in the corrosion resistance of the TC4 titanium alloy after ESD strengthening treatment, which

was attributed to the integrity of the coating surface. Kiryukhantsev et al. [47] combined magnetron sputtering with spark deposition technology and conducted a comparative study on Ti–C–Ni–Fe, Ti–C–Ni–Al, and double-layer Ti–C–Ni–Al/Ti–C–Ni–Fe coatings. The research indicated that employing the two-step combination technique allowed the production of dual-layer coatings consisting of Ti–C–Ni–Al/Ti–C–Ni–Fe, which exhibited a higher corrosion resistance than the deposited single-layer Ti–C–Ni–Al coatings. Research has shown that during the corrosion process, corrosion initially occurs from defects such as surface pores and microcracks, gradually affecting the entire surface. Therefore, improving the uniformity and density of the titanium alloy strengthening layer is crucial. Studies have demonstrated that eliminating pores and microcracks on the strengthened surface, and reducing and avoiding direct corrosion of the titanium alloy substrate can enhance the corrosion resistance of the strengthened surface [63]. Liu et al. [64] employed a rotating flexible copper electrode in conjunction with high-frequency pulse power to conduct spark surface strengthening on the surface of the titanium alloy. This resulted in a reaction between elements such as oxygen, nitrogen, and carbon in the air and the titanium alloy surface under the high-temperature and high-pressure conditions generated during discharge. The flexible electrode, composed of multiple metal wires, allowed the release of discharge energy through each wire, dispersing the energy of a single pulse. Furthermore, the mechanical rotation and scraping of the metal wires on the surface of the strengthening layer eliminated evident traditional discharge erosion pits. The presence of microcracks on the strengthening surface was reduced to some extent, enhancing the corrosion resistance and surface wear resistance of the strengthened surface. Shang et al. [65] utilized a surface modification technique that combined ultrasonic impact and spark deposition to modify the surface of a TC4 titanium alloy, resulting in the preparation of a dense modified layer with a thickness of approximately 11 μm . The study revealed that the modified layer on the surface of the TC4 titanium alloy mainly consisted of titanium oxide (Ti_2O_3), aluminum oxide (Al_2O_3), and a titanium–aluminum intermetallic compound (Al_3Ti). Although the self-corrosion potential of the modified layer was slightly higher than that of the TC4 titanium alloy substrate, its corrosion current density was significantly smaller, and the charge transfer resistance of the modified layer was greater than that of the TC4 titanium alloy. Hence, the modified layer exhibited better corrosion resistance compared to the TC4 titanium alloy substrate.

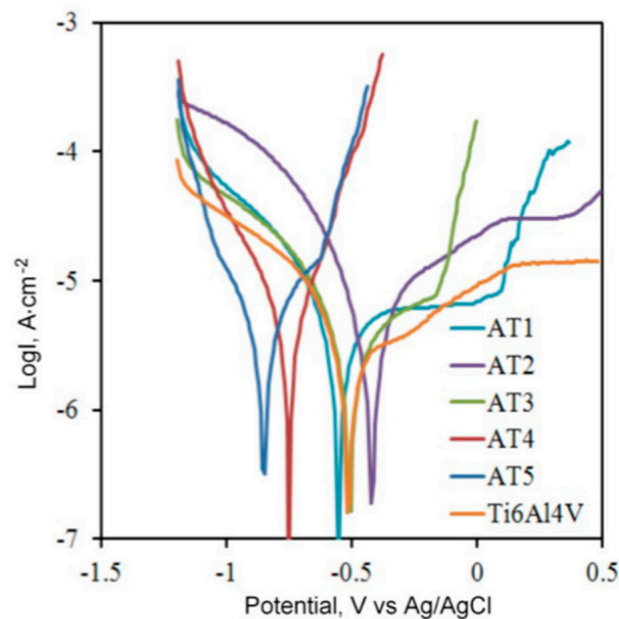


Figure 13. Polarization curves of coatings in 3.5% NaCl solution. Reprinted with permission from Ref. [36] Copyright 2020 Elsevier.

L. P. Kornienko et al. [66] employed the ESD method to enhance the strength of the alloy. Figure 14 depicts the relationship between the corrosion rate at 100 °C and the H₂SO₄ concentration for palladium deposited on a titanium surface using the ESD method. The results demonstrated that after ESD on the titanium surface, its corrosion resistance in a high-temperature sulfuric acid solution increased by 1–2 orders of magnitude. This was attributed to the presence of Pd and Ti–Pd intermetallic compounds in the coating, resulting in the passivation of titanium. The content of Pd in the alloy layer was found to be dependent on the discharge energy and discharge time. Furthermore, mechanical alloying significantly improved the corrosion resistance of titanium alloys compared to manual alloying, which was related to the higher and more uniform distribution of Pd in the surface layer. Mechanical alloying experiments conducted in vacuum, argon, and air revealed that the formation of coatings with the highest Pd enrichment occurred in an argon atmosphere. Lastly, after annealing at 1150 °C in a vacuum, the corrosion resistance of titanium increased by 2–2.5 times due to the more uniform distribution of Pd.

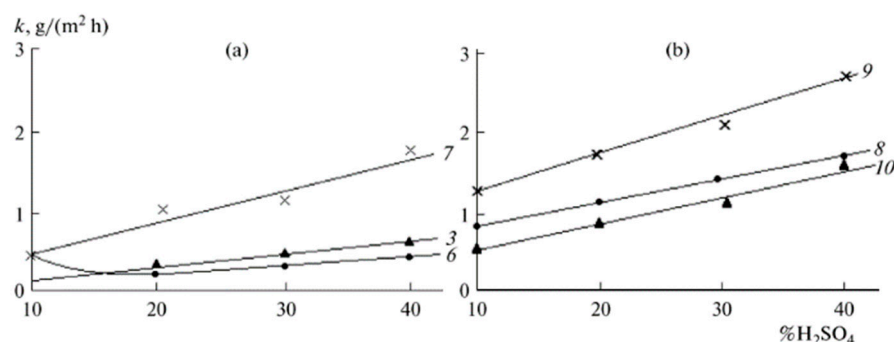


Figure 14. Corrosion rate of titanium with the electro spark palladium coatings versus the concentration of H₂SO₄ at 100 °C: (a) palladium coating under “mild” conditions; (b) palladium coating under “severe” conditions. The numbers of the curves correspond to the numbers of the specimens in Table 1. Curves 3, 6, 8, and 10 correspond to the specific time of alloying of 2 min/cm², and curves 7 and 9 to 4 min/cm². The test time was from 5 to 10 h. Reprinted with permission from Ref. [66] Copyright 2007 Springer Nature BV.

However, research on preparing corrosion-resistant coatings on titanium alloy surfaces using electrical discharge deposition technology is not yet extensive and in-depth. In the future, researchers will conduct in-depth studies on the physicochemical properties of oxide films in this field, as well as the homogeneity of coatings, in order to fill the gap in research findings and contribute to the application of electrical discharge deposition technology in the field of titanium alloys.

3.4. High Temperature Oxidation Resistance

Titanium alloys react with oxygen during service, resulting in decreased plasticity and embrittlement when the oxygen concentration is too high [67]. The formation of the metal oxide film follows the oxidation reaction mechanism proposed by Wagner [68]. The surface strengthening of titanium alloys through electrical discharge deposition technology can enhance their high-temperature oxidation resistance. For example, Burkov et al. [36] prepared coatings of an intermetallic Ti–Al compound on the surface of a Ti–6Al–4V alloy using electrical discharge treatment, and studied the kinetics of mass change of the coating samples and the Ti–6Al–4V alloy at a temperature of 900 °C (Figure 15). With an increase in aluminum concentration in the particle mixture, the phase composition of the corresponding coating changes from titanium-rich aluminides (Ti₃Al) to aluminum-rich aluminides (TiAl₃). The coating samples improve the oxidation resistance of the Ti–6Al–4V alloy at 900 °C by 1.1–3.4 times, with the highest aluminum content exhibiting the best oxidation resistance.

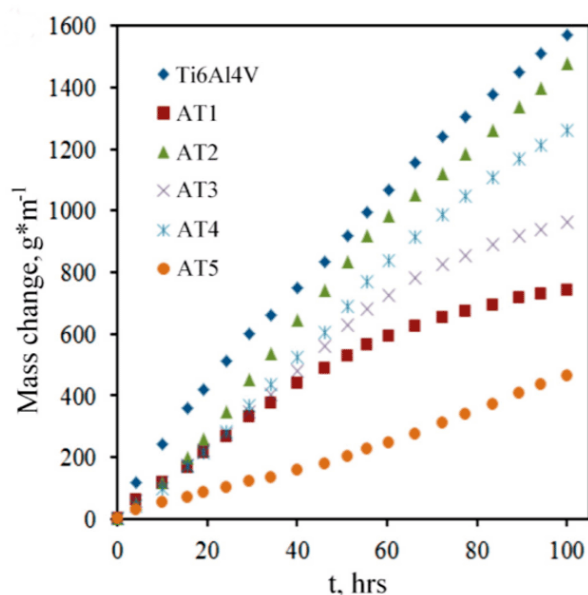


Figure 15. Cyclic oxidation resistance of coatings at 900 °C. Reprinted with permission from Ref. [36] Copyright 2020 Elsevier.

Li et al. [69] used electrical discharge deposition technology to prepare aluminum coatings on $\text{Ti}_3\text{Al} \pm \text{Nb}$ alloys to enhance their high-temperature oxidation resistance. The TiAl_3 coatings prepared on $\text{Ti}_3\text{Al} \pm \text{Nb}$ alloys were crack-free and metallurgically bonded to the substrate. Isothermal oxidation tests conducted in air at 800 °C and 900 °C indicated that the coatings exhibited lower oxidation rates and a good resistance to spalling. The reason for this can be attributed to the excellent oxide-forming ability of TiAl_3 , where the presence of a certain thickness of a TiAl_3 surface layer during the experimental process can generate a protective Al_2O_3 oxide layer. Al_2O_3 has a much lower growth rate than TiO_2 , thereby promoting and maintaining a lower oxidation rate of the aluminum oxide layer on the sample surface. Additionally, Du et al. [70] also demonstrated the higher oxidation resistance of Al_2O_3 films. Furthermore, oxidation occurs through the diffusion of oxygen atoms between the matrix material at high temperatures; therefore, the oxidation resistance is closely related to the morphology of the oxide film and the inherent structure of the titanium alloy. For lamellar structures, bimodal structures have more phase boundaries and grain boundary defects, where phase boundaries and grain boundaries serve as diffusion paths for oxygen, making oxygen interface diffusion easier in bimodal structures, resulting in severe oxidation [71]. For example, Long et al. [72] found that Ti-33Al-3Cr-0.5Mo alloys exhibited higher oxidation resistance when they had a lamellar structure. Leyens et al. [73] also demonstrated that titanium alloys with fine-layered microstructures have higher high-temperature oxidation resistance compared to coarse equiaxed grain titanium alloys. Similarly, Tang et al. [71] found that a Ti600 alloy with a lamellar microstructure exhibited higher oxidation resistance compared to bimodal structures. Dolgiy et al. [74], used the spark alloying method to prepare coatings on a TC11 alloy (Ti-6.5Al-3.5Mo-1.5Zr-0.3Si wt%). The oxidation behavior of the TC11 alloy and its deposited coatings in air at 700 °C was studied. The results showed that the coating prepared using Ni/TC11 had a high-temperature oxidation rate 1.4 times higher than that of the uncoated substrate. The coating prepared using Al/TC11 had the lowest oxidation rate (0.28 g/m^2), which was about two times lower than the oxidation rate of the TC11 alloy. Podchernyaeva et al. [75], used insoluble Ti and Zr nitride electrodes for strengthening treatment on the surface of a BT6 titanium alloy. They studied the mass transfer kinetics, distribution of alloying elements, and the performance after spark alloying of the VT6 titanium alloy surface. The test results showed that the microhardness of the alloyed layer was 3–5 times higher than that of the raw material, and the microhardness of the heat-affected zone was

1.5–2.0 times higher than that of the raw material. The coated samples also exhibited a significantly higher resistance to high-temperature oxidation. Li et al. [76]. used a simple and effective ESD method to prepare aluminum coatings on Ti₃Al and TiAl intermetallic compounds directly. The typical thickness of the coating was 15/20 μm, with gradient composition and metallurgical bonding to the substrate. Figure 16a shows the oxidation kinetics of the TiAl alloy at 900 °C. Isothermal oxidation tests in air at 800 °C and 900 °C for up to 300 h showed that the oxidation rates of all coated samples were much lower than that of the uncoated sample. Additionally, all coated samples exhibited excellent resistance to oxidation scale spalling, as shown in Figure 16b. Analytical analysis showed that the oxide film of the coated samples consisted mainly of dense alumina or corundum, while the oxidation products of the uncoated samples were mainly corundum. The results indicated that changes in oxide properties and microstructure played a key role in reducing oxidation rates and improving spalling resistance. Podchernyaeva et al. [77] investigated the formation mechanism, frictional characteristics, and high-temperature oxidation resistance of spark coatings on a VT6 alloy (Al 5.5%–7.0%, V 4.2%–6.0%). Tungsten-free, hard-alloy, spark-melting electrodes were prepared using powder metallurgy methods. A composite material structure was formed in the spark coatings. The VT6 alloy with spark alloying exhibited improved frictional performance and high-temperature oxidation resistance, as the oxidation thermogravimetric and differential thermal analysis curves were shifted to higher temperatures, significantly enhancing the alloy's tribological and oxidation-resistance properties.

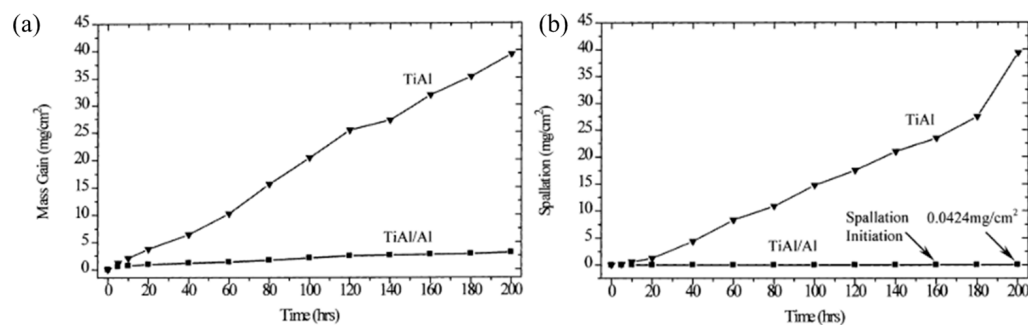


Figure 16. Oxidation kinetics and scale spallation of uncoated and ESD-coated TiAl at 900 °C in air; (a) total oxidation mass gain and (b) amount of spalled oxide. Reprinted with permission from Ref. [36] Copyright 2020 Elsevier.

Based on the above, it can be concluded that in the future, when addressing the high-temperature oxidation resistance issue of titanium alloys, it is advisable to incorporate alloying elements with high-temperature oxidation resistance into the design of titanium alloy compositions. This would enhance and stabilize the high-temperature oxidation resistance of titanium alloys after surface modification.

3.5. Biocompatibility

Titanium alloys have become the most attractive materials for biomedical applications due to their excellent mechanical properties, superior biocompatibility, and strong corrosion resistance. Table 1 presents the mechanical performance data of some titanium alloy implants [78]. However, limitations such as poor wear resistance, corrosion resistance [79], and unfavorable biological responses [80,81] have restricted their safe, reliable, and widespread use in clinical practice. Researchers have focused on finding surface modification techniques, including physical, chemical, and biological treatments, to enhance their bioactivity [82].

Table 1. Mechanical properties of partial medical titanium implants. Reprinted with permission from Ref. [78] Copyright 1998 Elsevier.

Implant Material	Microstructure	Ultimate Tensile Strength (MPa)	Elastic Modulus	Yield Strength (MPa)
Bone	Viscoelastic	90–140	10–30	10–40
CP-Ti	(α)	785	105	692
Ti–6Al–4V	($\alpha + \beta$)	960–970	110	850–900
Ti–6Al–7Nb	($\alpha + \beta$)	1024	105	921
Ti–5Al–2.5Fe	($\alpha + \beta$)	1033	110	914
Ti–12Mo–6Zr–2Fe	Metastable (β)	1060–1100	74–85	1000–1060
Ti–15Mo–5Zr–3Al	Metastable (β)/ aged ($\beta + \alpha$)	992–975/ 1099–1312	75/ 88–113	870–968/ 1087–1284
Ti–15Mo–2.8Nb–3Al	Metastable (β)/ aged ($\beta + \alpha$)	721/ 1310	82/ 100	771/ 1215
Ti–13Nb–13Zr	($\alpha' + \beta$)	1030	79	900
Ti–35Nb–7Zr–5Ta	Metastable (β)	590	55	530
Ti–35Nb–7Zr–5Ta–0.4O	Metastable (β)	1010	66	976

Surface modification techniques such as plasma spraying [83], physical vapor deposition [84], electrodeposition [85], and anodization [86] often encounter challenges related to poor bond strength. Surface-strengthening techniques like high-temperature nitriding [87] and sintering active ceramics [88] may compromise the properties of the substrate. In contrast, electrical spark deposition technology can overcome these drawbacks and is crucial for the surface modification of titanium and its alloys in medical implants. Table 2 provides a brief overview of the applications of electrical spark deposition technology in the surface modification of titanium and its alloys in the field of biomedicine [89–94].

Table 2. Biological application of ESD technology to surface modification of titanium and its alloys [89–94].

Workpiece	Surface Characterization		In Vivo or Vitro Study		Application
	SR/ μm	BRL	In Vivo	In Vitro	
Ti alloy [89]	7.8	TiO ₂ layer	×	Rabbit	Orthopedics
Ti alloy [90]	3.4	×	×	×	
Ti–6Al–4V [91]	1.8–3.2	Biocompatible 40- μm -thick TiC layer	×	MG–63 Cell line	Biomedical application or clinical uses
Si ₃ N ₄ –TiN [92]	1.4 \pm 0.15	Recast layer was found	×	Epithelial cells	Orthopedics
Nitinol [93]	×	Thin recast layer	×	×	Orthopedic implants
CP–Ti [94]	×	TiO ₂ , TiC biocompatible recast layer	×	×	Dental implants

Note: SR: surface roughness; BRL: biocompatibility layer; in vivo: in vivo experiment; in vitro: in vitro experiment.
×: This data was not available or the trial was not conducted.

Tang et al. [91] utilized electrical spark deposition technology with graphite as the electrode to produce coatings of approximately 40 μm on titanium alloy surfaces under different conditions: air, nitrogen atmosphere, and silicone oil. The experimental results showed that the main phase of the coatings was TiC. Compared to the coatings prepared in air and nitrogen atmospheres, the coatings produced in silicone oil demonstrated a denser and more perfect surface structure. Additionally, the surface-enhanced layer treated with silicone oil exhibited good biocompatibility and bioactivity, facilitating early cell adhesion on the substrate surface without significantly affecting cell proliferation. Prakash et al. [57] employed electrical spark deposition technology to the surface modification of β -Ti implants used in orthopedic applications. They obtained a hard surface layer containing

bio-ceramic oxides, carbides, and oxides, confirming that these three substances contribute to enhancing the biocompatibility of β -Ti alloys. Harcuba et al. [95] investigated the properties of a Ti-6Al-4V alloy after surface modification using electrical spark deposition. The prepared coatings exhibited macroscopic roughness. The biocompatibility of the Ti-6Al-4V samples subjected to surface treatment was studied using MG 63 cell cultures, and the results showed that the electrical-spark-deposition-modified samples provided a better growth substrate for cell adhesion, growth, and vitality compared to the TiO₂-coated surfaces. Therefore, electrical spark deposition treatment holds promise as a surface modification technique for orthopedic implants, facilitating good integration with surrounding bone tissue. A study by Strasky et al. [96] also demonstrated that the preparation of appropriate surface micro-, macro-, and nanostructures significantly enhances osteoblast differentiation and local factor production, promoting bone integration. Peng et al. [97] utilized an electrical spark deposition technique to create a nanoscale porous biocompatible surface with a roughness of 184 nm on a titanium alloy. The experimental results revealed that the formation of nanoscale ($\delta + \gamma$) hydrides played a crucial role in the formation of the nanoscale porous oxide layer, exerting a beneficial effect on osteoblast responses. Moreover, it is worth noting that the addition of active elements helps to improve the surface biological activity of titanium alloys. For example, the biological coatings containing Ti₃P and CaO prepared by Loginov et al. [98] have a controllable roughness and good biological activity. Furthermore, Yamaki et al. [99] studied in vivo bone biocompatibility. They manufactured biocompatible micro-surfaces with irregular spiral shapes using electrical spark deposition technology, achieving high bone integration capability. In addition, Litovchenko et al. [100] used Ti-C-Co-Ca₃(PO₄)₂-Ag-Mg electrodes to prepare a composite coating containing elemental Ag using the ESD technology, which has good antibacterial performance due to the presence of silver.

In conclusion, the application of ESD technology is particularly important for enhancing the biocompatibility of implants, as it not only transforms mechanically processed surfaces into controlled-thickness oxide and carbide layers to increase biocompatibility and generate hydrophilic surfaces, but it also has the capability to create nano-porous surfaces to enhance implant osseointegration. In recent years, the potential of ESD technology for producing biocompatible nano-porous surfaces on titanium and its alloys has been continuously explored. The surfaces prepared using ESD technology possess a layered morphology that provides a more suitable surface for osteoblast proliferation and for the improvement of implant fixation. This technology modifies the titanium surface with various types of oxides and alloying elements, enhancing corrosion resistance and wear resistance. Additionally, it can produce biocompatible porous oxide structures to promote cell growth and adhesion. Current research trends indicate that the oxide-carbide-porous layers formed via spark processing on titanium substrates enhance biological activity. The adaptability of titanium implants to bone tissue is a critical and important issue. In biomedical applications, surface modification is often required for implant fixation and long-term stability [101,102]. Electric spark processing can improve the surface properties and chemical characteristics of biomaterials. It holds the potential for processing biocompatible materials, ranging from metals or alloys to ceramics, and finds wide applications in fields such as dentistry, orthopedics, and microsurgery.

4. Summary and Outlook

The advantages of ESD technology, such as simple and convenient equipment operation, low cost, and significant material performance improvement, give it broad prospects for the surface treatment and modification of titanium alloys. However, many issues still need to be further addressed in practical applications. Firstly, due to the low precision of the equipment, the deposition layer thickness cannot be precisely controlled, resulting in limited layer thickness and difficulties in controlling surface roughness. Additionally, the equipment's simplicity leads to low efficiency and unstable processing techniques, resulting in low automation and reliability. Secondly, the application of ESD in the medical

field is still in its early stages, and its role in the surface modification of biomaterials is still experimental. The rapidly developing field of biomanufacturing faces significant challenges and opportunities. To address these shortcomings, researchers need to conduct further in-depth research related to the following aspects to improve the practicality of ESD technology:

- (1) Improving the automation level of this technology is a primary concern, as it can effectively enhance the production efficiency of ESD technology.
- (2) It is necessary to enhance ESD technology through optimizing various process parameters. The impact of multiple factors and parameters on material performance is highly complex, and there is enormous potential for enhancing material performance. In particular, the medium environment significantly influences ESD technology. Air atmosphere, argon gas, and nitrogen gas all affect ESD technology, as revealed in existing research. In the future, the application of ESD technology under different medium conditions, such as vacuum, water, and water vapor, can be further studied to address these exposed issues.
- (3) Further research is needed to deepen the study of ESD technology in the fields of corrosion resistance and biomedical applications. In-depth investigations should be conducted to explore the significant enhancements in corrosion resistance performance achieved by coatings prepared using ESD technology. Analyzing corrosion mechanisms and controlling the process parameters of ESD technology can enable the fabrication of highly corrosion-resistant and excellent biocompatible coatings.
- (4) Further strengthening of the present research on electric spark composite technology is needed. On the one hand, improvements can be achieved by developing new types of electrode materials, such as ceramics and composites, which can facilitate a better control of the deposition layer thickness. On the other hand, the research and development of composite coatings using different materials can effectively enhance the surface properties of materials by utilizing the deposition layer selected for material performance improvement.

Author Contributions: Conceptualization, J.W. and L.Z.; methodology, J.W.; software, S.D.; validation, J.W. and M.Z.; formal analysis, S.D.; investigation, M.Z.; resources, L.Z.; data curation, M.Z.; writing—original draft preparation, J.W.; writing—review and editing, J.W. and M.Z.; visualization, S.D.; supervision, L.Z.; project administration, L.Z.; funding acquisition, J.W. and L.Z. All authors have read and agreed to the published version of the manuscript.

Funding: This research was funded by the Zhejiang Province Key Research and Development Plan Project (2023C01082), and the Agricultural Science and Technology Key R & D Program of Taizhou (NYJBGS202201).

Institutional Review Board Statement: This review does not need ethical approval.

Informed Consent Statement: This review does not involve human experiments.

Data Availability Statement: No new data are created in this review.

Conflicts of Interest: The authors declare no conflict of interest.

References

1. Hong, X.; Feng, K.; Tan, Y.F.; Wang, X.; Tan, H. Effects of process parameters on microstructure and wear resistance of TiN coatings deposited on TC11 titanium alloy by electro spark deposition. *Trans. Nonferrous Met. Soc. China* **2017**, *27*, 1767–1776. [[CrossRef](#)]
2. Bai, H.Q.; Zhong, L.S.; Kang, L.; Liu, J.; Zhuang, W.; Lv, Z.; Xu, Y. A review on wear-resistant coating with high hardness and high toughness on the surface of titanium alloy. *J. Alloys Compd.* **2021**, *882*, 160645. [[CrossRef](#)]
3. Khanan, N.; Davim, J.P. Design-of-experiments application in machining titanium alloys for aerospace structural components. *Measurement* **2015**, *61*, 280–290. [[CrossRef](#)]
4. Schauerte, O. Titanium in automotive production. *Adv. Eng. Mater.* **2003**, *5*, 411–418. [[CrossRef](#)]
5. Cheng, J.; Li, F.; Zhu, S.; Yu, Y.; Qiao, Z.; Yang, J. Electrochemical corrosion and tribological evaluation of TiAl alloy for marine application. *Tribol. Int.* **2017**, *115*, 483–492. [[CrossRef](#)]

6. Tawancy, H.M. On the hydrogen embrittlement of commercially pure alpha titanium: An example from the petrochemical industry. *J. Mater. Eng. Perform.* **2017**, *26*, 504–513. [[CrossRef](#)]
7. Chen, Q.Z.; Thouas, A.G. Metallic implant biomaterials. *Mater. Sci. Eng. R Rep.* **2015**, *87*, 1–57. [[CrossRef](#)]
8. Yuan, S.; Lin, N.; Zou, J.; Lin, X.; Liu, Z.; Yu, Y.; Wang, Z.; Zeng, Q.; Chen, Q.; Tian, L.; et al. In-situ fabrication of gradient titanium oxide ceramic coating on laser surface textured Ti–6Al–4V alloy with improved mechanical property and wear performance. *Vacuum* **2020**, *176*, 109327. [[CrossRef](#)]
9. Zhao, Y.; Fan, Z.; Tan, Q.; Yin, Y.; Lu, M.; Huang, H. Interfacial and tribological properties of laser deposited TiO_xN_y/Ti composite coating on Ti alloy. *Tribol. Int.* **2020**, *155*, 106758. [[CrossRef](#)]
10. Halada, G.P.; Clayton, C.R. The intersection of design, manufacturing and surface engineering. In *Handbook of Environmental Degradation of Materials*; William Andrew Publishing: Norwich, NY, USA, 2005; pp. 321–344.
11. Kong, L.; Wang, X.; He, Q.; Han, J.; Zhang, S.; Ding, K.; Liu, Z. Microcosmic mechanism of die-sinking mixed-gas atomization discharge ablation process on titanium alloy. *Int. J. Adv. Manuf. Technol.* **2021**, *117*, 949–960. [[CrossRef](#)]
12. Cadney, S.; Brochu, M. Formation of amorphous Zr_{41.2}Ti_{13.8}Ni₁₀Cu_{12.5}Be_{22.5} coatings via the electro spark deposition process. *Intermetallics* **2007**, *16*, 518–523. [[CrossRef](#)]
13. Myslyvchenko, O.M.; Gaponava, O.P.; Tarelnyk, V.B.; Krapivka, M.O. The structure formation and hardness of high-entropy alloy coatings obtained by electro spark deposition. *Powder Metall. Met. Ceram.* **2020**, *59*, 201–208. [[CrossRef](#)]
14. Pei, H.; Wang, J.; Li, Z.; Li, Z.; Yao, X.; Wen, Z.; Yue, Z. Oxidation behavior of recast layer of air-film hole machined by EDM technology of Ni-based single crystal blade and its effect on creep strength. *Surf. Coat. Technol.* **2021**, *419*, 12728. [[CrossRef](#)]
15. Johnson, R.N.; Sheldon, G.L. Advances in the electrospark deposition coating process. *J. Vac. Sci. Technol. A Vac. Surf. Film.* **1986**, *4*, 2740–2746. [[CrossRef](#)]
16. Barile, C.; Casavola, C.; Pappaletta, G.; Renna, G. Giovanni Pappaletta. Advancements in electrospark deposition (ESD) technique: A short review. *Coatings* **2022**, *12*, 1536. [[CrossRef](#)]
17. Chen, Z.X. *Electro Spark Surface Strengthening Technology*; China Machine Press: Beijing, China, 1987. (In Chinese)
18. Zhang, G.C. Electric spark hardening tool. *Met. Work. (Met. Cut.)* **1985**, *10*, 19–20. (In Chinese)
19. Zhu, Z.X.; Zhang, X.P.; Yang, X. Devising of new kind of equipment of pulse electro spark hardening. *J. Tsinghua Univ. (Sci. Technol.)* **1999**, *39*, 33–35. (In Chinese)
20. Wang, Z.M.; Huang, S.S.; Zhang, Z.L. A study of spark hardening process. *China Surf. Eng.* **2000**, *13*, 19–21. (In Chinese)
21. Norbert, R.; Konrad, B. Laser treatment of electro-spark coatings deposited in the carbon steel substrate with using nanostructured WC–Cu electrodes. *Phys. Procedia* **2012**, *39*, 295–301.
22. Radek, N.; Bartkowiak, K. Laser treatment of Cu–Mo electro-spark deposited coatings. *Phys. Procedia* **2011**, *12*, 499–505. [[CrossRef](#)]
23. Chen, Z.; Zhou, Y. Surface modification of resistance welding electrode by electro-spark deposited composite coatings: Part I. Coating characterization. *Surf. Coat. Technol.* **2006**, *201*, 1503–1510. [[CrossRef](#)]
24. Wang, Z.Q.; Wang, X.R. Microstructure and flame-retardant properties of ti-cu coating on TC11 prepared via electrospark deposition. In Proceedings of the 2015 International Conference on Material Engineering and Mechanical Engineering (MEME2015), Istanbul, Turkey, 22–23 August 2015.
25. Koshuro, V.; Fomina, M.; Fomine, A.; Rodionov, I. Metal oxide (Ti, Ta)–(TiO₂, TaO) coatings produced on titanium using electro spark alloying and modified by induction heat treatment. *Compos. Struct.* **2018**, *196*, 1–7. [[CrossRef](#)]
26. Wang, D.; Gao, J.; Deng, S.; Wang, W. A novel particle planting process based on electrospark deposition. *Mater. Lett.* **2022**, *306*, 130872. [[CrossRef](#)]
27. Manakova, O.S.; Kudryashov, A.E.; Levashov, E.A. On the application of dispersion-hardened SHS electrode materials based on (Ti, Zr)C carbide using electrospark deposition. *Surf. Eng. Appl. Electrochem.* **2015**, *51*, 413–421. [[CrossRef](#)]
28. Burkov, A.A. The effect of discharge pulse energy in electrospark deposition of amorphous coatings. *Prot. Met. Phys. Chem. Surf.* **2022**, *58*, 1018–1027. [[CrossRef](#)]
29. Li, C.; Ge, P.; Bi, W. Thermal simulation of the single discharge for electro-spark deposition diamond wire saw. *Int. J. Adv. Manuf. Technol.* **2021**, *114*, 3597–3604. [[CrossRef](#)]
30. Frangini, S.; Masci, A. A study on the effect of a dynamic contact force control for improving electrospark coating properties. *Surf. Coat. Technol.* **2010**, *204*, 2613–2623. [[CrossRef](#)]
31. Lešnjak, A.; Tušek, J. Processes and properties of deposits in electrospark deposition. *Sci. Technol. Weld. Join.* **2002**, *7*, 391–396. [[CrossRef](#)]
32. Jin, B.D.; Zhao, W.S.; Cao, G.H.; Wang, Z.L.; Xiao, K. Fabrication of micro structure using EDM deposition. *Mater. Sci. Forum* **2006**, *532–533*, 305–308. [[CrossRef](#)]
33. Frangini, S.; Masci, A.; Bartolomeo, A.D. Cr₇C₃-based cermet coating deposited on stainless steel by electro spark process: Structural characteristics and corrosion behavior. *Surf. Coat. Technol.* **2002**, *149*, 279–286. [[CrossRef](#)]
34. Agarwal, A.; Dahotre, N.B. Synthesis of boride coating on steel using high energy density processes. *Mater. Charact.* **1999**, *42*, 31–44. [[CrossRef](#)]
35. Zhang, R.; Li, J.; Yan, D.; Zhao, Y. Mechanical properties of WC–8Co wear-resistant coating on pump impellers surface by electro-spark. *Rare Met. Mater. Eng.* **2015**, *44*, 1587–1590.
36. Burkov, A.A.; Chigrin, P.G. Synthesis of Ti–Al intermetallic coatings via electro spark deposition in a mixture of Ti and Al granules technique. *Surf. Coat. Technol.* **2020**, *387*, 125550. [[CrossRef](#)]

37. Jin, X.; Ye, P.; Ji, H.; Suo, Z.; Wei, B.; Li, X.; Fang, W. Oxidation resistance of powder metallurgy Ti–45Al–10Nb alloy at high temperature. *Int. J. Miner. Metall. Mater.* **2022**, *29*, 2232–2240. [[CrossRef](#)]
38. Yin, K.; Bian, X.; Han, N.; Yao, Y.; Zhou, J. Effect of the addition of Al–Ti–C master alloy on the microstructure and microhardness of a cast Al–10Mg alloy. *J. Univ. Sci. Technol. Beijing* **2006**, *13*, 149–153. [[CrossRef](#)]
39. Ntasi, A.; Mueller, W.D.; Eliades, G.; Zinelis, S. The effect of Electro Discharge Machining (EDM) on the corrosion resistance of dental alloys. *Dent. Mater. Off. Publ. Acad. Dent. Mater.* **2010**, *26*, 237–245. [[CrossRef](#)] [[PubMed](#)]
40. Geng, M.; Wang, W.; Zhang, X. Microstructures and properties of Ni/Ti (C, N) composite cermet coating prepared by electrospark deposition. *Surf. Technol.* **2020**, *49*, 222–229.
41. Liu, Y.; Wang, D.; Deng, C.; Huo, L.; Wang, L.; Fang, R. Novel method to fabricate Ti–Al intermetallic compound coatings on Ti–6Al–4V alloy by combined ultrasonic impact treatment and electrospark deposition. *J. Alloys Compd. Interdiscip. J. Mater. Sci. Solid–State Chem. Phys.* **2015**, *628*, 208–212. [[CrossRef](#)]
42. Shafyei, H.; Salehi, M.; Bahrami, A. Fabrication, microstructural characterization and mechanical properties evaluation of Ti/TiB/TiB₂ composite coatings deposited on Ti6Al4V alloy by electro–spark deposition method. *Ceram. Int.* **2020**, *46*, 15276–15284. [[CrossRef](#)]
43. Zamulaeva, E.I.; Levashov, E.A.; Sviridova, T.A.; Shvyndina, N.; Petrzhik, M. Pulsed electrospark deposition of MAX phase Cr2AlC based coatings on titanium alloy. *Surf. Coat. Technol.* **2013**, *235*, 454–460. [[CrossRef](#)]
44. Wang, R.J.; Qian, Y.Y.; Liu, J. Structural and interfacial analysis of WC92–Co8 coating deposited on titanium alloy by electrospark deposition. *Appl. Surf. Sci. J. Devoted Prop. Interfaces Relat. Synth. Behav. Mater.* **2004**, *228*, 405–409. [[CrossRef](#)]
45. Hong, X.; Tan, Y.; Zhou, C.; Xu, T.; Zhang, Z. Microstructure and tribological properties of Zr–based amorphous–nanocrystalline coatings deposited on the surface of titanium alloys by electrospark deposition. *Appl. Surf. Sci.* **2015**, *356*, 1244–1251. [[CrossRef](#)]
46. Wang, Y.M.; Zhang, P.F.; Guo, L.X.; Ouyang, J.H.; Zhou, Y.; Jia, D.C. Effect of microarc oxidation coating on fatigue performance of Ti–Al–Zr alloy. *Appl. Surf. Sci.* **2009**, *255*, 8648–8653. [[CrossRef](#)]
47. Kiryukhantsev–Korneev, P.V.; Sheveyko, A.N.; Shvindina, N.V.; Levashov, E.A.; Shtansky, D.V. Comparative study of Ti–C–Ni–Al, Ti–C–Ni–Fe, and Ti–C–NiAl/Ti–C–Ni–Fe coatings produced by magnetron sputtering, electro–spark deposition, and a combined two–step process. *Ceram. Int.* **2018**, *44*, 7637–7646. [[CrossRef](#)]
48. Sun, K.W.; Yu, H.; Wu, G.Y. Interface behavior of NiCr coating deposited on TA2 surface by EDM. *Weld. Technol.* **2015**, *44*, 10–12. (In Chinese)
49. Liu, Y.; Wang, T.; Su, Q.; Ma, F.; Yang, D.; Zhnag, S. Experimental study on NiCr–3 coating on titanium alloy surface by electro–spark deposition (ESD). *Aeronaut. Manuf. Technol.* **2022**, *65*, 104–112. (In Chinese)
50. Hao, J.J.; Peng, H.B.; Huang, J.H. TiN/Ti composite coating deposited on titanium alloy surface by reactive EDM. *Trans. China Weld. Inst.* **2009**, *30*, 69–72. (In Chinese)
51. Su, G.Q.; You, T.; Zhang, C.H. Research on depositing Ni45 alloy on titanium alloy surface by electro spark deposition. *China Foundry* **2008**, *5*, 244–248.
52. Liu, Y.; Wang, D.; Deng, C.; Huo, L.; Wang, L.; Cao, S. Feasibility study on preparation of coatings on Ti–6Al–4V by combined ultrasonic impact treatment and electrospark deposition. *Mater. Des.* **2014**, *63*, 488–492. [[CrossRef](#)]
53. Burkov, A.A.; Zaikova, E.R.; Dvornik, M.I. Deposition of Ti–Ni–Zr–Mo–Al–C composite coatings on the Ti6Al4V alloy by electrospark alloying in a granule medium. *Surf. Eng. Appl. Electrochem.* **2018**, *63*, 18–26. [[CrossRef](#)]
54. Hong, X.; Tan, Y.F.; Wang, X.L.; Tan, H.; Xu, T. Effects of nitrogen flux on microstructure and tribological properties of in–situ TiN coatings deposited on TC11 titanium alloy by electrospark deposition. *Trans. Nonferrous Met. Soc. China* **2015**, *25*, 3329–3338. [[CrossRef](#)]
55. Hong, X.; Tan, Y.; Wang, X.; Wang, X.; Xu, T.; Gao, L. Microstructure and wear resistant performance of TiN/Zr–base amorphous–nanocrystalline composite coatings on titanium alloy by electrospark deposition. *Surf. Coat. Technol.* **2016**, *305*, 67–75. [[CrossRef](#)]
56. Li, P.; Qiao, S.R.; Zhang, L.L. Ti17 alloy surface modification by electrospark deposition with silicon bronze electrode. *Trans. Mater. Heat Treat.* **2008**, *29*, 148–152. (In Chinese)
57. Prakash, C.; Kansal, H.K.; Pabla, B.S.; Puri, s. Potential of silicon powder–mixed electro spark alloying for surface modification of β –phase titanium alloy for orthopedic applications. *Mater. Today Proc.* **2017**, *4*, 10080–10083. [[CrossRef](#)]
58. Li, C.B.; Chen, D.H.; Chen, W.W.; Wang, L.; Luo, D. Corrosion behavior of TiZrNiCuBe metallic glass coatings synthesized by electro spark deposition. *Corros. Sci.* **2014**, *84*, 96–102. [[CrossRef](#)]
59. Hashimoto, K.; Park, P.-Y.; Kim, J.-H.; Yoshioka, H.; Mitsui, H.; Akiyama, E.; Habazaki, H.; Kawashima, A.; Asami, K.; Grzesik, Z.; et al. Recent progress in corrosion-resistant metastable alloys. *Mater. Sci. Eng. A* **1995**, *198*, 1–10. [[CrossRef](#)]
60. Ferreira, E.A.; Rocha–filho, R.C.; Biaggio, S.R.; Bocchi, B. Corrosion resistance of the Ti–50Zr at.% alloy after anodization in different acidic electrolytes. *Corros. Sci.* **2010**, *52*, 4058–4063. [[CrossRef](#)]
61. Teplenko, M.A.; Podchernyaeva, I.A.; Panasyuk, A.D. Structure and wear resistance of coatings on titanium alloy and steels obtained by electro spark alloying with AlN–ZrB₂ material. *Powder Metall. Met. Ceram.* **2002**, *41*, 154–161. [[CrossRef](#)]
62. Tang, C.B.; Liu, D.X.; Wang, Z. Electro–spark strengthened titanium alloy surfaces by using silicon electrode and their wear resistance properties. *Mech. Sci. Technol. Aerosp. Eng.* **2011**, *30*, 226–232. (In Chinese)
63. Mahbub, M.R.; Kovach, L.; Wolfe, A.; Lalvani, S.; James, P.F.; Jahan, M.P. Enhancing cell adhesion and corrosion performance of titanium alloy by surface and sub–surface engineering using WEDM. *Surf. Coat. Technol.* **2021**, *429*, 127929. [[CrossRef](#)]

64. Liu, Z.; Xu, A.; Wang, Z.; Zhang, Y. Surface property of titanium strengthening of alloys by electrospark surface flexible electrode. *J. Nanjing Univ. Aeronaut. Astronaut.* **2012**, *44*, 222–227.
65. Jin, S.; Wei, C.; Chen, Y.C. Effect of ultrasonic impact combined with electrospark deposition surface Treatment on corrosion resistance of TC4 titanium alloy. *Corros. Prot.* **2021**, *42*, 22–25. (In Chinese)
66. Kornienko, L.P.; Chernova, G.P.; Mihailov, V.V.; Gitlevich, A.E. Use of the electrospark alloying method to increase the corrosion resistance of a titanium surface. *Surf. Eng. Appl. Electrochem.* **2011**, *47*, 9–17. [[CrossRef](#)]
67. Feng, X.; Liang, Y.; Sun, H.; Wang, S. Effect of dislocation slip mechanism under the control of oxygen concentration in alpha-case on strength and ductility of TC4 alloy. *Metals* **2021**, *11*, 1057. [[CrossRef](#)]
68. Wagner, C. Formation of composite scales consisting of oxides of different metals. *J. Electrochem. Soc.* **1956**, *103*, 627. [[CrossRef](#)]
69. Li, Z.W.; Gao, W.; He, Y.D. Protection of a Ti₃Al±Nb alloy by electro-spark deposition coating. *Scr. Mater.* **2001**, *45*, 1099–1105. [[CrossRef](#)]
70. Du, H.L.; Aljarany, A.; Datta, P.K.; Burnell-Gray, J.S. Oxidation behaviour of Ti–46.7Al–1.9W–0.5Si in air and Ar–20%O₂ between 750 and 950 °C. *Corros. Sci.* **2005**, *47*, 1706–1723. [[CrossRef](#)]
71. Tang, H.F. Study on the Microstructure and High Temperature Properties of Ti600 Alloy. Ph.D. Thesis, Northeastern University, Shenyang, China, 2010. (In Chinese).
72. Long, Y.Y.; Liang, Y.; Fu, G.Y. Effect of MA and addition agents on the high temperature oxidation resistance and microstructure of TiAl alloys. *Titan. Ind. Prog.* **2004**, *2*, 27–29. (In Chinese)
73. Leyens, C.; Peters, M.; Kaysser, W.A. Influence of microstructure on oxidation behaviour of near-α titanium alloys. *Mater. Sci. Technol.* **2013**, *12*, 213–218. [[CrossRef](#)]
74. Dolgiy, Z.O.; Shao, W.Z.; Kozyr, A.V.; Martynov, S.V. Formation of two-layer heat-resistant coatings on TC11 alloy by electro-spark alloying method. *Adv. Mater. Res.* **2012**, *538*, 175–180. [[CrossRef](#)]
75. Podchernyaeva, I.A.; Lavrenko, V.A.; Berezanskaya, V.I.; Smirnov, V.P. Electrospark alloying of the titanium alloy VT6 with tungsten-free hard alloys. *Powder Metall. Met. Ceram.* **1996**, *35*, 588–591. [[CrossRef](#)]
76. Li, Z.; Gao, W.; Yoshihara, M.; He, Y. Improving oxidation resistance of Ti₃Al and TiAl intermetallic compounds with electro-spark deposit coatings. *Mater. Sci. Eng. A* **2003**, *347*, 243–252. [[CrossRef](#)]
77. Podchernyaeva, I.; Juga, A.I.; Berezanskaya, V.I. Properties of electrospark coatings on titanium alloy. *Key Eng. Mater.* **1997**, *132*, 1507–1510. [[CrossRef](#)]
78. Long, M.; Rack, H.J. Titanium alloys in total joint replacement—a materials science perspective. *Biomaterials* **1998**, *19*, 1621–1639. [[CrossRef](#)]
79. Da, S.L.; Ueda, M.; Silva, M.; Codaro, E.N. Corrosion behavior of Ti–6Al–4V alloy treated by plasma immersion ion implantation process. *Surf. Coat. Technol.* **2007**, *201*, 8136–8139.
80. Anselme, K.; Bigerelle, M. Topography effects of pure titanium substrates on human osteoblast long-term adhesion. *Acta Biomater.* **2005**, *1*, 211–222. [[CrossRef](#)] [[PubMed](#)]
81. Zhu, X.L.; Chen, J.; Scheideler, L.; Reichl, R.; Geis-Gerstorf, J. Effects of topography and composition of titanium surface oxides on osteoblast responses. *Biomaterials* **2003**, *25*, 4087–4103. [[CrossRef](#)] [[PubMed](#)]
82. Zhecheva, A.; Malinov, S.; Sha, W. Titanium alloys after surface gas nitriding. *Surf. Coat. Technol.* **2006**, *201*, 2467–2474. [[CrossRef](#)]
83. Zheng, X.B.; Huang, M.H.; Ding, C.X. Bond strength of plasma-sprayed hydroxyapatite/Ti composite coatings. *Biomaterials* **2000**, *21*, 841–849. [[CrossRef](#)]
84. Chu, P.K.; Chen, J.Y.; Wang, L.P.; Huang, N. Plasma-surface modification of biomaterials. *Mater. Sci. Eng. R* **2002**, *36*, 143–206. [[CrossRef](#)]
85. Probst, J.; Gbureck, U.; Thull, R. Binary nitride and oxynitride PVD coatings on titanium for biomedical applications. *Surf. Coat. Technol.* **2001**, *148*, 226–233. [[CrossRef](#)]
86. Liu, C.; Bi, Q.; Matthews, A. Tribological and electrochemical performance of PVD TiN coatings on the femoral head of Ti–6Al–4V artificial hip joints. *Surf. Coat. Technol.* **2003**, *163*, 597–604. [[CrossRef](#)]
87. Xiao, X.F.; Liu, R.F.; Zheng, Y.Z. Hydroxyapatite/titanium composite coating prepared by hydrothermal-electrochemical technique. *Mater. Lett.* **2005**, *59*, 1660–1664. [[CrossRef](#)]
88. García, C.; Ceré, S.; Durán, A. Bioactive coatings prepared by sol-gel on stainless steel 316L. *J. Non-Cryst. Solids* **2004**, *348*, 218–224. [[CrossRef](#)]
89. Wennerberg, A.; Hallgren, C.; Johansson, C.; Sawase, C.; Lausmaa, J. Surface characterization and biological evaluation of spark-eroded surfaces. *J. Mater. Sci.* **1997**, *8*, 757–763.
90. Murali, M.; Yeo, S.H. Rapid biocompatible microdevice fabrication by micro electro-discharge machining. *Biomed. Microdevices* **2004**, *6*, 41–45. [[CrossRef](#)]
91. Tang, C.B.; Liu, D.X.; Wang, Z.; Yang, G. Electro-spark alloying using graphite electrode on titanium alloy surface for biomedical applications. *Appl. Surf. Sci.* **2011**, *257*, 6364–6371.
92. Bucciotti, F.; Mazzocchi, M.; Bellosi, A. Perspectives of the Si₃N₄-TiN ceramic composite as a biomaterial and manufacturing of complex-shaped implantable devices by electrical discharge machining (EDM). *J. Appl. Biomater. Funct. Mater.* **2010**, *8*, 28–32.
93. Theisen, W.; Schuermann, A. Electro discharge machining of nickel-titanium shape memory alloys. *Mater. Sci. Eng. A* **2003**, *378*, 200–204. [[CrossRef](#)]

94. Zinelis, S.; Jabbari, Y.A.; Thomas, A.; Silikas, S.; Eliades, G. Multitechnique characterization of CPTi surfaces after electro discharge machining (EDM). *Clin. Oral Investig.* **2014**, *18*, 67–75. [[CrossRef](#)]
95. Harcuba, P.; Bacakova, L.; Strasky, J.; Bacakova, M.; Janecek, M. Surface treatment by electric discharge machining of Ti–6Al–4V alloy for potential application in orthopaedics. *J. Mech. Behav. Biomed. Mater.* **2012**, *7*, 96–105. [[CrossRef](#)] [[PubMed](#)]
96. Strasky, J.; Havlikova, J.; Bacakova, L.; Harcuba, P.; Mhaede, M.; Janecek, M. Characterization of electric discharge machining, subsequent etching and shot-peening as a surface treatment for orthopedic implants. *Appl. Surf. Sci.* **2013**, *281*, 73–78. [[CrossRef](#)]
97. Peng, P.W.; Ou, K.L.; Lin, H.C.; Pan, Y.N.; Wang, C.H. Effect of electrical discharging on formation of nanoporous biocompatible layer on titanium. *J. Alloys Compd.* **2010**, *492*, 625–630. [[CrossRef](#)]
98. Loginov, P.A.; Levashov, E.A.; Potanin, A.Y.; Kudryashov, A.E.; Manakova, O.S.; Shvyndina, N.V.; Sukhorukova, I.V. Sintered Ti–Ti₃P–CaO electrodes and their application for pulsed electrospark treatment of titanium. *Ceram. Int.* **2016**, *42*, 7043–7053. [[CrossRef](#)]
99. Yamaki, K.; Kataoka, Y.; Ohtsuka, F.; Miyazaki, T. Micro-CT evaluation of in vivo osteogenesis at implants processed by wire-type electric discharge machining. *Dent. Mater. J.* **2012**, *31*, 427–432. [[CrossRef](#)]
100. Litovchenko, N.V.; Potanin, A.Y.; Zamulaeva, E.I.; Sukhorukova, I.V.; Pogozhev, Y.S.; Gloushankova, N.A.; Ignatov, S.G.; Levashov, E.A.; Shtansky, D.V. Combustion synthesis of Ti–C–Co–Ca₃(PO₄)₂–Ag–Mg electrodes and their utilization for pulsed electrospark deposition of bioactive coatings having an antibacterial effect. *Surf. Coat. Technol.* **2017**, *309*, 75–85. [[CrossRef](#)]
101. Zhang, M.; Xue, Y.; Huang, X.; Ma, D.; Yu, S.; Zhu, L.; Wu, Y. Cytocompatibility and osteogenic activity of Ta–Ti–O nanotubes anodically grown on Ti6Al4V alloy. *Appl. Surf. Sci.* **2023**, *614*, 156165. [[CrossRef](#)]
102. Zhang, M.; Zhu, L.; Wang, J.; Ye, N.; Dai, S.; Yu, S.; Wu, Y. Surface modification of biomedical metals by double glow plasma surface alloying technology: A review of recent advances. *J. Mater. Res. Technol.* **2023**, *24*, 3423–3452. [[CrossRef](#)]

Disclaimer/Publisher’s Note: The statements, opinions and data contained in all publications are solely those of the individual author(s) and contributor(s) and not of MDPI and/or the editor(s). MDPI and/or the editor(s) disclaim responsibility for any injury to people or property resulting from any ideas, methods, instructions or products referred to in the content.